JNC TJ7400 2003-006

放射性塩素同位体比（$^{36}Cl/Cl$）に基づく地球化学解析

（核燃料サイクル開発機構　契約業務報告書）

2003年3月

三菱商事株式会社

放射性塩素同位体比（$^{36}Cl/Cl$）に基づく地球化学解析

要旨

Richard Metcalfe※

本報告書は、平成14年度に実施された塩素の放射性同位体である^{36}Clについての研究成果に関するものである。この研究結果は、^{36}Clデータにより地下水の起源及び経路を解釈することができる可能性を示唆している。

^{36}Cl分析のため、東濃地域から4試料の地下水と1試料の温泉水が採取されている。地下水は瑞浪超深地層研究所用地内の試錐孔（MSB-2号孔、MSB-4号孔）から採取され、温泉水は鬼岩温泉（小松屋）から採取されたものである。また、東濃地域との比較のため、幌延の試錐孔(HDB-1号孔)から採取された地下水も分析した。

岩石の化学特性に関するデータおよび物理検層結果を地層中の$^{36}Cl/Cl$の理論的平衡値を求めるために用いた。これらは、地下水サンプルで測定された結果と比較することができ、以下の事柄について知見を得ることができる。

- 地下水が岩石中に十分長く留まっていたか
- 地下水中に溶解している塩素の混合の空間的な規模

また、岩石の化学データと物理検層結果を用い、既存のデータであるMIU-4号孔、KNA-6号孔およびDH-12号孔の^{36}Clデータの解析をおこなった。

MIU-4号孔で採取された地下水の$^{36}Cl/Cl$比の値は、花崗岩中における平衡状態下のものではなかったことが考えられる。また試錐孔の上部では^{36}Cl量が等質であることが示されている。一方、DH-12号孔のデータは、比較的長い滞留時間を有し、花崗岩中での平衡状態下での地層中における^{36}Cl生成を反映したものであると考えられる。

堆積岩の下部から得られた地下水試料のうち一つの分析結果は、花崗岩における分析結果と類似していた。一方、物理検層で測定されたガンマ線のデータは、土岐夾炭累層の下層では、より高い^{36}Cl生成量が示唆されている。このことから、花崗岩からClが上方へ移動している可能性が示唆される。

MSB-孔の物理検層データは、地層中における^{36}Cl生成量が均一ではないことを示唆しており、地下水の^{36}Clデータが地下水流動を評価する上で非常に役に立つ可能性がある。

MSB-2号孔でのClは調査区間（深さ79 mから176 m）において良く混合している。本孔において、深さ120m以浅の地下水の$^{36}Cl/Cl$比はこの深度において平衡状態のものではないと考えられるため、Clはより深部に位置していたと想定される。

MSB-2号孔において、花崗岩中の平衡状態での^{36}Clを有する地下水が堆積岩の下部に上昇した場合、地下水の$^{36}Cl/Cl$が堆積岩中の^{36}Cl生成量の不均一性を反映するまでに有する滞留時間は数万年程度である。

$^{36}Cl/Cl$を用いて地球化学解析をおこなうにあたり、地層中における^{36}Cl生成の不均一性の規模に比べ採水区間が長い場合には、$^{36}Cl/Cl$の深度依存性を同定できない可能性があり、採水区間がこの空間的な不均一性の規模より短いことが必要である。採水区間を短くできない場合、地下水の^{36}Clデータを得る手法の1つとして、岩芯から得られる抽出水及び岩芯の溶出試験により得られる水を用いることが挙げられる。

本報告書は、三菱商事株式会社が核燃料サイクル開発機構との契約により実施した業務成果に関するものである。

機構担当課室：東濃地科学センター　瑞浪超深地層研究所　研究グループ
※株式会社クインテッサジャパン

A hydrochemical investigation using $^{36}Cl/Cl$ in groundwaters

Abstract

Richard Metcalfe*

This report describes ^{36}Cl studies which were undertaken during the H14 financial year. The results of this study suggest that, if ^{36}Cl data can be obtained for groundwaters at spatial scales comparable with, or smaller than, the spatial scales of the variability in *in-situ* ^{36}Cl production in the host rock, the data could potentially be useful for interpreting groundwater origins and flow paths.

Four groundwater samples and one onsen water sample from the Tono area were collected for ^{36}Cl analysis. The groundwater samples came from boreholes MSB-2 and MSB-4 in the MIU Construction Site, whereas the onsen water was taken from Oniiwa Onsen (Komatsuya). In addition, a single sample from borehole HDB-1 at Horonobe was also sent for analysis.

Supporting rock chemical data and wireline geophysical data have also been evaluated, to provide a basis for interpreting the ^{36}Cl data. Rock analyses and spectral gamma wireline data were used to estimate theoretical limiting equilibrium $^{36}Cl/Cl$ ratios in the rock. These have been compared with the compositions measured for groundwater samples, enabling a judgement to be made as to:

- whether the waters have resided for long enough in the rock to approach equilibrium (> c. 1.5 Ma);
- the spatial scales of mixing of the dissolved Cl in the groundwater.

The estimates of *in-situ* $^{36}Cl/Cl$ production made with the newly available rock chemical data and wireline geophysical data have enabled ^{36}Cl data obtained previously from MIU-4, KNA-6 and DH-12 during H12 and H13 to be interpreted more confidently.

In particular it seems that $^{36}Cl/Cl$ ratios measured previously in groundwater samples from MIU-4 are not in equilibrium with *in-situ* production in the granite. Furthermore, they imply that the Cl is homogenised, at least on the scale of the upper half of the borehole. In contrast, the data from DH-12 imply that the Cl could be in equilibrium with *in-situ* ^{36}Cl production in the granite, which would be consistent with a relatively long residence time. An analysis of a groundwater sample from the lower sedimentary rocks is similar to analyses in the granite, in spite of the fact that wireline gamma data imply higher ^{36}Cl production in the lower Toki Lignite-bearing Formation. This may indicate upward movement of Cl from the granite.

The wireline data from the MSB-boreholes suggest that there could be significant contrasts in *in-situ* ^{36}Cl production between different locations. This suggests the possibility that the ^{36}Cl data to be obtained for groundwater sampled from these boreholes, may be useful for evaluating groundwater flow.

In MSB-2, the groundwater Cl appears to be well-mixed over the sampled interval, between 79 m to 176 m depth. In this borehole, the groundwater Cl cannot have equilibrated with the *in-situ* ^{36}Cl production above 120 m depth. Instead, the Cl probably originated at greater depths.

If water containing Cl equilibrated with the mean in-situ neutron flux in the granite moved upwards into the lower sedimentary rocks in MSB-2, the water would subsequently need to remain stationary for several tens of thousands of years to produce observable spatial variations in $^{36}Cl/Cl$ ratios.

Some of the groundwater sampling intervals are wide compared to the spatial scale of variability in in-situ production and therefore variations in natural $^{36}Cl/Cl$ may not be resolved. Future sampling should focus on obtaining groundwater samples from intervals smaller than the spatial scale over which in-situ ^{36}Cl production varies. A possible complimentary

approach to sampling groundwaters would be to analyse ^{36}Cl in leachates and squeezed porewaters obtained from core samples.

This work was performed by Mitsubishi Corporation under construct with Japan Nuclear Cycle Development Institute.
JNC Liaison: Underground Research Group, Mizunami Underground Research Laboratory, Tono Geoscience Center
* Quintessa Ltd.

Table of contents

Tables

Figures

1 Introduction

This report describes the acquisition of additional data for ^{36}Cl from new boreholes that were drilled in the Tono area, Gifu ken and at Horonobe, Hokkaido, during the H14 financial year. The principle aim was to assess the value of these data for constraining groundwater flow models. To allow the ^{36}Cl data to be interpreted as fully as possible it was also aimed to obtain supporting information concerning the composition of the rocks and groundwaters, to be used to estimate the natural *in-situ* production rates of ^{36}Cl in the subsurface. The new interpretations build on previous interpretations that were based on a small number of groundwater ^{36}Cl analyses obtained previously in H12 and H13.

2 Approach

2.1 Theory of ^{36}Cl applications

Applications of ^{36}Cl analyses in hydrogeology are covered by an increasingly large literature (e.g. Phillips et al., 1986; Andrews et al. 1986; Andrews et al. 1989; Andrews et al., 1994).

At depths greater than a few metres (typically around 20 m), the main source of *in-situ* ^{36}Cl production in the water is usually the neutron activation of stable ^{35}Cl. In this case, the *in-situ* neutron flux results from radioactive decay processes in the rock. In addition ^{36}Cl will be produced in the rock matrix, and released subsequently by water/rock interactions. This is likely to be important when the waters are relatively fresh and/or the rock contains relatively abundant Cl-bearing minerals (e.g. micas in acid igneous rocks and halite in evaporites). In cases where such water/rock interactions have occurred significantly, it will usually be impossible to use the ^{36}Cl data to estimate a meaningful residence time for the water, though it may be possible place limits on this residence time.

2.2 Calculation of *in-situ* ^{36}Cl production

To evaluate the relative importance of mixing and in-situ production of ^{36}Cl, in-situ equilibrium $^{36}Cl/Cl$ ratios must be estimated. This can be done in one of three main ways:

- by using direct measurements of the natural neutron flux to calculate ^{36}Cl production rates;
- by using knowledge of rock chemistry to calculate a theoretical neutron flux and hence ^{36}Cl production;
- by identifying correlations between $^{36}Cl/Cl$ ratios and the U and Th contents of the rocks.

Natural neutron fluxes have not been measured during the Tono investigations and therefore the first method was not used in the present work. However, both the other methods were employed.

In applying the second approach, chemical analyses of the rocks were used in conjunction with equations and approaches described in (Andrews et al., 1986) and (Andrews et al., 1989).

The third approach makes use of the fact that, for any given rock type, small variations in the concentrations of chemical components other than U and Th have a relatively small effect on

the calculated $^{36}Cl/Cl$ ratios. Here, the relationships between U and Th concentrations and $^{36}Cl/Cl$ ratios suggested by Lehmann and Loosli (1991) were employed as follows:

$$\phi = 10^{-5} \times (\alpha[U] + \beta[Th]) \qquad \text{Equation 2.2.1}$$

where: ϕ is the neutron flux in neutrons $cm^{-2}\,s^{-1}$, [U] and [Th] are concentrations in the rock of U and Th, in ppm, and α and β are constants, depending upon the rock types as given in Table 1.

Table 1. Constants α and β, for use in calculating in-situ neutron fluxes according to the equation of Lehmann and Loosli (1991).

	α	β
Granite	0.86	0.3
Sandstone	0.56	0.16
Limestone	1.07	0.28

The equilibrium $^{36}Cl/Cl$ ratio is then calculated from:

$$\frac{^{36}Cl}{Cl} = \phi \times 4.55 \times 10^{-10} \qquad \text{Equation 2.2.2}$$

This approach can be used when there are insufficient whole-rock data to allow calculations of neutron fluxes to be made easily.

2.3 Sample selection

Four groundwater samples were collected from two boreholes in the MIU Construction Site, at Mizunami, Gifu ken. These boreholes mainly intersect the Miocene sedimentary rocks of the Mizunami Group, but also penetrate the uppermost Tertiary Toki Granite. It was expected that the lower sedimentary rocks would be relatively rich in uranium compared to shallower and deeper rocks, reflecting the proximity of the Tsukiyoshi uranium ore deposit. It was also thought likely that the granite would in turn contain more uranium than the shallower sedimentary rocks. As a result of these variations in rock chemistry, there was considered to be potential for large variations in the *in-situ* production of ^{36}Cl, which correlates strongly with the amount of U (and associated Th) present in the rock.

For comparison, a single fresh water sample, taken from the Oniiwa Onsen (Komatsuya) was also sent for analysis. It was anticipated that this water would give additional insights into the $^{36}Cl/Cl$ ratios of groundwater that has been relatively recently recharged.

Finally, a single sample from borehole HDB-1 at Horonobe was also sent for analysis. This sample has an Na-Cl dominated chemistry and is much more saline than any of the Tono samples. It was therefore planned to use this sample for comparison.

Sample details are summarised in Tables 2. and 3.

2.4 Sample analysis

Groundwater samples were sent for analysis to the Purdue Rare Isotope Measurement Laboratory (PRIME lab) at the University of Purdue in Indiana, U.S.A. This laboratory is a recognised leader in the analysis of cosmogenic isotopes such as ^{36}Cl. The analyses were performed by Accelerator Mass Spectrometry (AMS) (described in (Elmore and others., 1993) and in the web page http://primelab.physics.purdue.edu/). This method uses a particle accelerator in conjunction with ion sources, large magnets, and detectors, to separate out interferences and count single atoms in the presence of $1x10^{15}$ (a thousand million million) stable atoms.

Table 2. Summary descriptions of Tono samples sent for ^{36}Cl analysis.

Sample No	Sample Description	Approx Cl Content mg/l	Volume Sent to PrimeLab litres	Split Sent to PrimeLab[1]	Borehole	Depth mabh	Formation Sampled
MSB279/1	Fresh Groundwater	155	1	1	MSB-2	79.0-130.5	Toki Lignite-Bearing Formation
MSB2132/1	Fresh Groundwater	223	1	1	MSB-2	132.0-154.0	Toki Lignite-Bearing Formation (basal congolomerate)
MSB2172/1	Fresh Groundwater	189	1	1	MSB-2	171.5-175.5	Toki Granite - Upper Weathered Zone
MSB496/1	Fresh Groundwater	96	1	1	MSB-4	95.5-99.0	Toki Granite - Fresh Granite[2]
KOM0715	Fresh Onsen Water	5.4	3	1,2,3	Komatsuya	-	

Table 3. Summary description of the Horonobe sample sent for ^{36}Cl analysis.

Sample No	Sample Description	Approx Cl Content mg/l	Volume Sent to PrimeLab litres	Split Sent to PrimeLab	Borehole	Depth mabh	Formation Sampled
HDB1548	Saline Groundwater	8920	1	All Sent	HDB-1	548.0-563.18	Wakkanai Formation

2.5 Supporting information

The principal types of supporting information used during the project were:

- whole-rock analyses from boreholes DH-12, MIU-4 and KNA-6;
- spectral gamma wireline data from boreholes MSB-1, MSB-2, MSB-3 and MSB-4;
- natural gamma logs from boreholes DH-12, MIU-4 and KNA-6;
- chemical analyses of groundwaters from these boreholes.

3 Results

3.1 ^{36}Cl/Cl analyses

All the presently available ^{36}Cl analyses for the Tono area are summarised in Table 4 and are plotted in Figure 1. The comparative data obtained from Horonobe borehole HDB-1 are tabulated in Table 5.

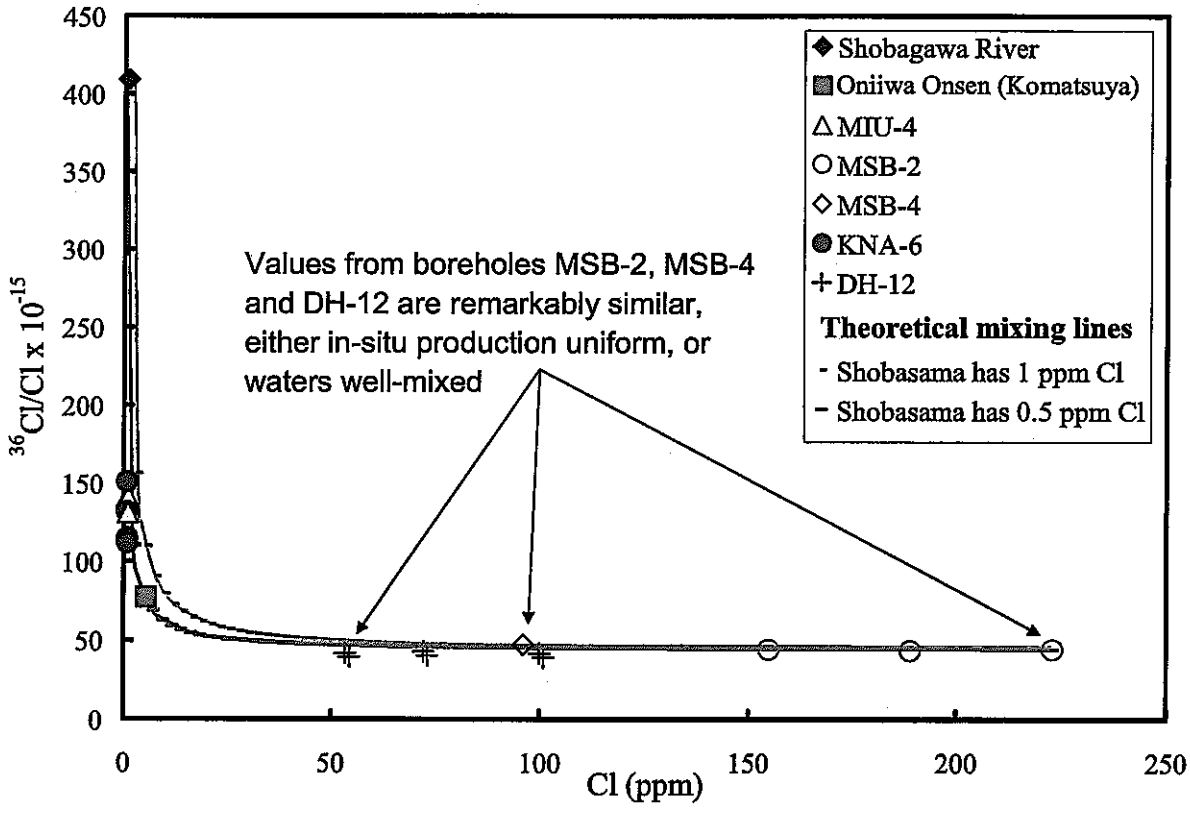

Figure 1. ^{36}Cl/Cl ratios plotted against Cl concentration for groundwater samples from the Tono area. The theoretical mixing lines are constructed between the Shobasama river water and the groundwater sample with the highest Cl content, from between 132.0 and 154.0 m in borehole MSB-2.

Table 4. Summary of ^{36}Cl data for the Tono onsen waters and groundwaters, obtained during the present study and previously, during H12 and H13. Halide analyses of these waters are also given.

Water Description	Location	Depth		Depth		Elevation		Rock Formation	$^{36}Cl/Cl$		Cl		Br		F	
		mabh		mbgl		masl			Atomic Ratio x 10^{-15}		ppm		ppm		ppm	
		Min	Max	Min	Max	Min	Max		Estimate	2σ Error	Estimate	2σ Error	Estimate	2σ Error	Estimate	2σ Error
Shobagawa River Water	Shobasama-site, Shobagawa river	0	0	0	0	c. 210	c. 210	Runs over Akeyo Formation	409	36	1	N.R.	N.R.	N.R.	N.R.	N.R.
KOM0715	Oniiwa Onsen (Komatsuya)	0	0	0	0	N.R.	N.R.	N.R.	77.4	6.4	5.4	N.R.	<0.1	N.R.	7.5	N.R.
MIU-4 Water	Borehole MIU-4	82.50	88.65	71.45	76.77	145.54	140.22	Toki Lignite-bearing Formation	131	16	1.03	0.02	<0.1	0.02	6.67	0.02
MIU-4 Water	Borehole MIU-4	95.02	134.47	82.29	116.45	134.70	100.54	Toki Granite	141	14	0.86	0.02	<0.1	0.01	11.05	0.01
MIU-4 Water	Borehole MIU-4	314.95	316.95	272.75	274.49	-55.76	-57.50	Toki Granite	141	18	1.07	0.02	<0.1	0.02	11.95	0.02
MSB-2	Borehole MSB-2	79.00	130.50	79.00	130.49	119.49	68.00	Toki Lignite-bearing Formation	44.3	5.0	155	N.R.	0.29	N.R.	11	N.R.
MSB-2	Borehole MSB-2	132.00	154.00	131.99	153.99	66.50	44.50	Toki Lignite-bearing Formation (basal congolomerate)	44.3	5.8	223	N.R.	0.42	N.R.	8.3	N.R.

Table 4. continued.

Water Description	Location	Depth		Depth		Elevation		Rock Formation	$^{36}Cl/Cl$		Cl		Br		F	
		mabh		mbgl		masl			Atomic Ratio x 10^{-15}		ppm		ppm		ppm	
		Min	Max	Min	Max	Min	Max		Estimate	2σ Error	Estimate	2σ Error	Estimate	2σ Error	Estimate	2σ Error
MSB-2	Borehole MSB-2	171.50	175.50	171.49	175.49	27.00	23.00	Lignite/Toki Granite – U. Weathered Zone	43.4	4.4	189	N.R.	0.25	N.R.	8.0	N.R.
MSB-4	Borehole MSB-4	95.50	99.00	95.50	99.00	118.95	115.45	Toki Granite - Fresh Granite	47.2	4.6	96	N.R.	0.18	N.R.	12	N.R.
Water TLG/1 - Duplicate 1	Borehole KNA-6	43.50	46.00	157.76	159.53	129.10	127.33	Granite/ Sediment	151	14	0.795	N.R.	<0.2	N.R.	4.35	N.R.
Water TLG/1 - Duplicate 2	Borehole KNA-6	43.50	46.00	157.76	159.53	129.10	127.33	Granite/ Sediment	132	14	0.795	N.R.	<0.2	N.R.	4.35	N.R.
Water G-1	Borehole KNA-6	50.5	101.00	162.71	198.42	124.15	88.44	Granite	115	14	0.845	N.R.	<0.2	N.R.	3.73	N.R.
Water G-2	Borehole KNA-6	50.5	101.00	162.71	198.42	124.15	88.44	Granite	112.1	11.8	0.845	N.R.	<0.2	N.R.	3.73	N.R.
DH-12 Water	Borehole DH-12	157.45	164.12	157.45	164.12	-20.07	-26.74	Toki Lignite-bearing Formation (congolomerate)	42	12	53.3	N.R.	<0.2	N.R.	14.8	N.R.
DH-12 Water	Borehole DH-12	279.40	344.67	279.40	344.67	-142.02	-207.29	Granite	41.6	11	99.9	N.R.	<0.2	N.R.	10.0	N.R.
DH-12 Water	Borehole DH-12	431.42	472.50	431.42	472.50	-294.04	-335.12	Granite	43	20	72.1	N.R.	<0.2	N.R.	12.8	N.R.

Table 5. Summary of ^{36}Cl data for the Horonobe HDB-1 groundwater, obtained during the present study. Halide analyses of this water are also given.

Water Description	Location	Depth		Depth		Elevation		Lithology	$^{36}Cl/Cl$		Cl		Br		F	
		mabh		mbgl		masl			Atomic Ratio x 10^{-15}		ppm		ppm		ppm	
		Min	Max	Min	Max	Min	Max		Estimate	2σ Error	Estimate	2σ Error	Estimate	2σ Error	Estimate	2σ Error
HDB-1 Water	Horonobe, Borehole HDB-1	548.0	563.18	548.0	563.18	-478.90	-494.08	Siliceous mudrock (Wakkanai Formation)	3.3	2.2	8920	N.R.	<0.1	N.R.	<0.1	N.R.

3.2 Theoretical equilibrium $^{36}Cl/Cl$ ratios

Theoretical equilibrium $^{36}Cl/Cl$ ratios, that should be approached by Cl dissolved in water with a residence time in the rock of more than about 1.5 Ma, have been calculated using rock analyses from boreholes MIU-4, DH-12 and HDB-1. These values are summarised in Tables 6 and 7. For rock samples corresponding most closely in space to sampled groundwaters, all the available chemical data were used, together with the equations of Andrews et al. (1986), Andrews et al. (1989) and Andrews et al. (1994). Owing to lack of data for key constituents, notably certain trace elements (particularly Cl), several different calculations were made, based on different assumptions about a rock's chemistry.

In addition, the approach of Lehmann and Loosli (1991) was also employed for these samples. This method was also used to calculate equilibrium $^{36}Cl/Cl$ ratios for all the other rock samples in each of these boreholes, so as to gain a better insight into the spatial variability of ^{36}Cl production.

In the cases of the MSB-series boreholes, there are presently no whole-rock analyses. However, there are spectral gamma wireline data, which indicate the concentrations of uranium and thorium effectively continuously down each borehole. These data were used in conjunction with the equations of Lehmann and Loosli (1991) to calculate theoretical equilibrium $^{36}Cl/Cl$ ratios. The results of these calculations are presented in Figures 2, 3, 4 and 5.

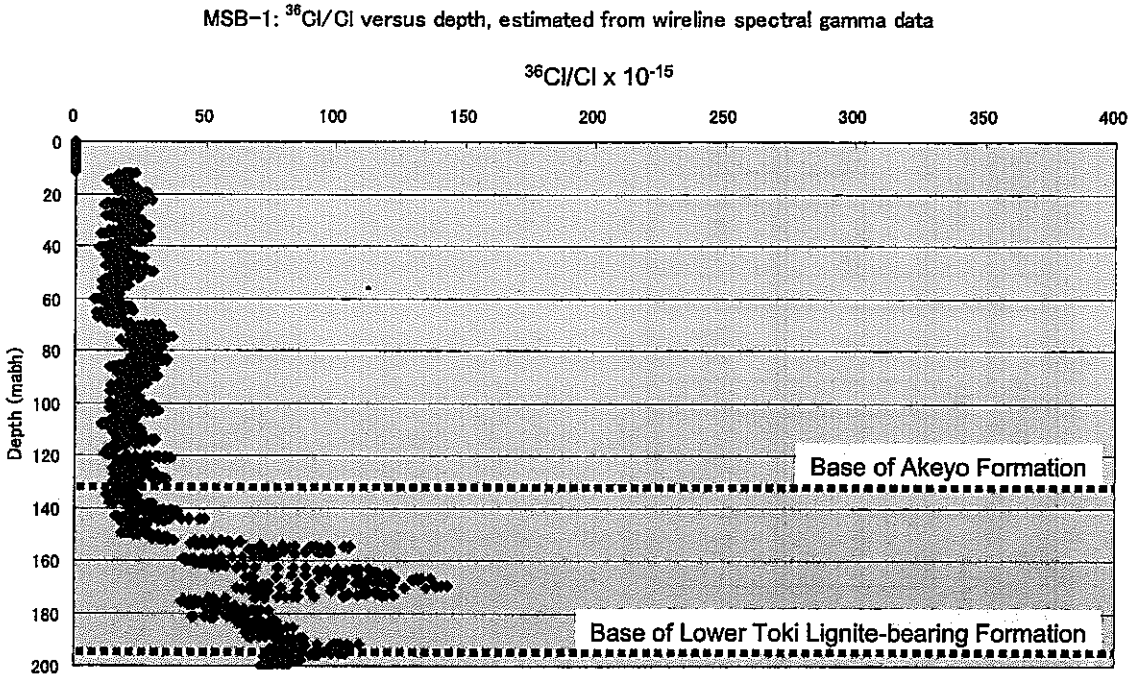

Figure 2. Theoretical equilibrium $^{36}Cl/Cl$ ratios calculated for borehole MSB-1, using spectral gamma wireline data and the approach of Lehmann and Loosli (1991).

Table 6. Summary of estimated maximum equilibrium $^{36}Cl/Cl$ ratios made using two different methods and a variety of constraints.

Borehole No.	Sample No.	Rock Type	Depth	Estimated maximum equilibrium $^{36}Cl/Cl$ in the rock matrix, made using the equations of Andrews et al. (1989)				Rock composition	$^{36}Cl/Cl$ from method of Lehmann & Loosli (1991)
				Cl content of rock ($mgkg^{-1}$)					
				200	1	200	1		
				$^{36}Cl/Cl$ (rock constituents lacking data constrained as given to right)		$^{36}Cl/Cl$ (rock constituents lacking data negligible)			
			mbgl	$x10^{-15}$		$x10^{-15}$			$x10^{-15}$
Tono, DH-12	None Given	Toki Granite	181.15	34	182	56	301	As in Appendix A, but no data for Cr, Co, Ni, Sm, Gd, Be, N, Li, B: Stripa Granite (left) or negligible (right) values used.	48
Tono, DH-12	None Given	Toki Granite	272.60	31	175	51	290	As in Appendix A, but no data for Cr, Co, Ni, Sm, Gd, Be, N, Li, B: Stripa Granite (left) or negligible (right) values used.	44
Tono, DH-12	None Given	Toki Granite	289.48	15	86	25	143	Apart from U and Th, other rock chemistry is as used for the 272.6 m sample	21
Tono, DH-12	None Given	Toki Granite	301.18	27	121	46	204	As in Appendix A, but no data for Cr, Co, Ni, Sm, Gd, Be, N, Li, B: Stripa Granite (left) or negligible (right) values used.	39
Tono, DH-12	None Given	Toki Granite	314.45	17	76	29	128	Apart from U and Th, other rock chemistry is as used for the 301.18 m sample	24
Tono, DH-12	None Given	Toki Granite	330.40	22	101	36	172	As in Appendix A, but no data for Cr, Co, Ni, Sm, Gd, Be, N, Li, B: Stripa Granite (left) or negligible (right) values used.	30

Grey indicates a rock sample from **within** a hydraulic test interval that yielded a groundwater sample for ^{36}Cl analysis.
Yellow indicates a rock sample from **outside** hydraulic test intervals that yielded groundwater samples for ^{36}Cl was analysis.
These rocks are chosen to bracket test intervals for which there are no rock data.

Table 6. Continued

Borehole No.	Sample No.	Rock Type	Depth	Estimated maximum equilibrium $^{36}Cl/Cl$ in the rock matrix, made using the equations of Andrews et al. (1989)				Rock composition	$^{36}Cl/Cl$ from method of Lehmann & Loosli (1991)
				Cl content of rock ($mgkg^{-1}$)					
				200	1	200	1		
				$^{36}Cl/Cl$ (rock constituents lacking data constrained as given to right)		$^{36}Cl/Cl$ (rock constituents lacking data negligible)			
			mbgl	$x10^{-15}$		$x10^{-15}$			$x10^{-15}$
Tono, DH-12	None Given	Toki Granite	348.65	12	59	21	99	Apart from U and Th, other rock chemistry is as used for the 330.4 m sample	17
Tono, DH-12	None Given	Toki Granite	369.95	27	126	46	213	As in Appendix A, but no data for Cr, Co, Ni, Sm, Gd, Be, N, Li, B: Stripa Granite (left) or negligible (right) values used.	37
Tono, DH-12	None Given	Toki Granite	420.15	43	210	70	348	As in Appendix A, but no data for Cr, Co, Ni, Sm, Gd, Be, N, Li, B: Stripa Granite (left) or negligible (right) values used.	59
Tono, DH-12	None Given	Toki Granite	435.80	28	153	45	251	As in Appendix A, but no data for Cr, Co, Ni, Sm, Gd, Be, N, Li, B: Stripa Granite (left) or negligible (right) values used.	38
Tono, DH-12	None Given	Toki Granite	450.25	23	116	37	196	As in Appendix A, but no data for Cr, Co, Ni, Sm, Gd, Be, N, Li, B: Stripa Granite (left) or negligible (right) values used.	31
Tono, DH-12	None Given	Toki Granite	465.25	38	214	61	348	No data for Cr, Co, Ni, Sm, Gd, Be, N, Li, B: Stripa Granite (left) or negligible (right) values used.	51
Tono, DH-12	None Given	Toki Granite	479.85	23	115	39	192	No data for Cr, Co, Ni, Sm, Gd, Be, N, Li, B: Stripa Granite (left) or negligible (right) values used.	33

Table 6. Continued

Borehole No.	Sample No.	Rock Type	Depth	Estimated maximum equilibrium $^{36}Cl/Cl$ in the rock matrix, made using the equations of Andrews et al. (1989)				Rock composition	$^{36}Cl/Cl$ from method of Lehmann & Loosli (1991)
				Cl content of rock ($mgkg^{-1}$)					
				200	1	200	1		
				$^{36}Cl/Cl$ (rock constituents lacking data constrained as given to right)		$^{36}Cl/Cl$ (rock constituents lacking data negligible)			
			mbgl	$x10^{-15}$		$x10^{-15}$			$x10^{-15}$
Tono, MIU-4	GM#1	Medium grained Bt-granite. Weathering : Moderately weathered (□). Alteration:Partially Bt altered to Chl(2p), Pl to clay minerals (2p)	97.42	38	172	40	179	As in Appendix A, but no data for B, N, C; Stripa Granite (left) or negligible (right) values used.	37
Tono, MIU-4	GM#2	Medium grained Bt-granite. Weathering : Fresh (□~□). Alteration: Partially Bt altered to Chl(1~2p), Pl to clay minerals (1~2p)	140.87	34	169	59	294	As in Appendix A, but no data for Sm, Gd, N, B, C; Stripa Granite (left) or negligible (right) values used.	45
Tono, MIU-4	GM#5	Medium grained Bt-granite. Weathering : Weathered entirely (□). Alteration : Hematite occurred. Most of Bt altered to Chl (3p), Pl to clay minerals (3p)	289.75	24	290	39	220	As in Appendix A, but no data for Sm, Gd, N, B; Stripa Granite (left) or negligible (right) values used.	32
Tono, MIU-4	GM#6	Medium grained Bt-granite. Weathering : Fresh (□). Alteration : Partially Bt altered to Chl(1~2p), Pl to clay minerals (1~2p)	340.12	46	241	77	405	As in Appendix A, but no data for Sm, Gd, N, B; Stripa Granite (left) or negligible (right) values used.	61

Table 6. Continued

Borehole No.	Sample No.	Rock Type	Depth	Estimated maximum equilibrium $^{36}Cl/Cl$ in the rock matrix, made using the equations of Andrews et al. (1989)				Rock composition	$^{36}Cl/Cl$ from method of Lehmann & Loosli (1991)
				Cl content of rock ($mgkg^{-1}$)					
				200	1	200	1		
				$^{36}Cl/Cl$ (rock constituents lacking data constrained as given to right)		$^{36}Cl/Cl$ (rock constituents lacking data negligible)			
			mbgl	$x10^{-15}$		$x10^{-15}$			$x10^{-15}$
Tono, MIU-4	WEZ# 1—1— ①	Greenish white clay	48.11	148	756	228	1172	As in Appendix A, but no data for Sm, Gd, N, B; Stripa Granite (left) or negligible (right) values used.	235
Tono, MIU-4	WEZ# 1—2	Weathered wallrock. Hydrothermal (epidote) alteration	96.26	87	423	139	685	As in Appendix A, but no data for Sm, Gd, N, B; Stripa Granite (left) or negligible (right) values used.	118
Tono, MIU-4	WCF# 1—1	Damaged zone (Cataclasite~ Fault breccia)	116.40	33	205	34	212	As in Appendix A, but no data for N, B; Stripa Granite (left) or negligible (right) values used.	48
Tono, MIU-4	WCF# 1—2	Fault core: (Cataclasite, Highly hydrothermal alteration, clay rich part, incohesive)	117.11	29	152	30	157	As in Appendix A, but no data for N, B; Stripa Granite (left) or negligible (right) values used.	43
Tono, MIU-4	WCF# 1—3 ①	Damaged zone	117.27	30	159	31	165	As in Appendix A, but no data for N, B; Stripa Granite (left) or negligible (right) values used.	43
Tono, MIU-4	WCF# 1—4	Damaged zone (Fault breccia, incohesive)	118.10	66	402	68	417	As in Appendix A, but no data for N, B; Stripa Granite values used.	70

Table 6. Continued

Borehole No.	Sample No.	Rock Type	Depth	Estimated maximum equilibrium $^{36}Cl/Cl$ in the rock matrix, made using the equations of Andrews et al. (1989)				Rock composition	$^{36}Cl/Cl$ from method of Lehmann & Loosli (1991)
				Cl content of rock ($mgkg^{-1}$)					
				200	1	200	1		
				$^{36}Cl/Cl$ (rock constituents lacking data constrained as given to right)		$^{36}Cl/Cl$ (rock constituents lacking data negligible)			
			mbgl	$x10^{-15}$		$x10^{-15}$			$x10^{-15}$
Horonobe, HDB-1	None Given	Wakkanai Formation	551.47	6	17	17	46	As in Appendix A, but no data for C, Cl, F, Cr, Co, Ni, Be, N, Li, B, mean shale (left) or negligible (right) values used.	Not Calculated
Horonobe, HDB-1	None Given	Wakkanai Formation	556.425	6	17	17	39	As in Appendix A, but no data for trace elements, including U and Th. Only major elements changed from values used in 551.42-551.52 m calculation	Not Calculated

Table 7. Summary statistics for estimates of $^{36}Cl/Cl$ made by the approach of Lehmann and Loosli (1991)

	Estimates from whole-rock chemistry				Estimates from wireline data			
	DH-13	MIU-4	DH-12	All Values	MSB-1	MSB-2	MSB-3	MSB-4
	$^{36}Cl/Cl$ x 10^{-15}	$^{36}Cl/Cl$ x 10^{-15}	$^{36}Cl/Cl$ x 10^{-15}	$^{36}Cl/Cl$ x 10^{-15}	$^{36}Cl/Cl$ x 10^{-15}	$^{36}Cl/Cl$ x 10^{-15}	$^{36}Cl/Cl$ x 10^{-15}	$^{36}Cl/Cl$ x 10^{-15}
Mean	31.47	54.46	31.77	36.88	35.59	33.01	74.10	43.17
Standard Deviation	9.48	42.50	11.97	24.21	27.78	22.83	45.82	58.13
Number	55	30	45	130	1886	1676	1941	906
Relative Standard Deviation (%)	30	78	38	66	78	69	62	135

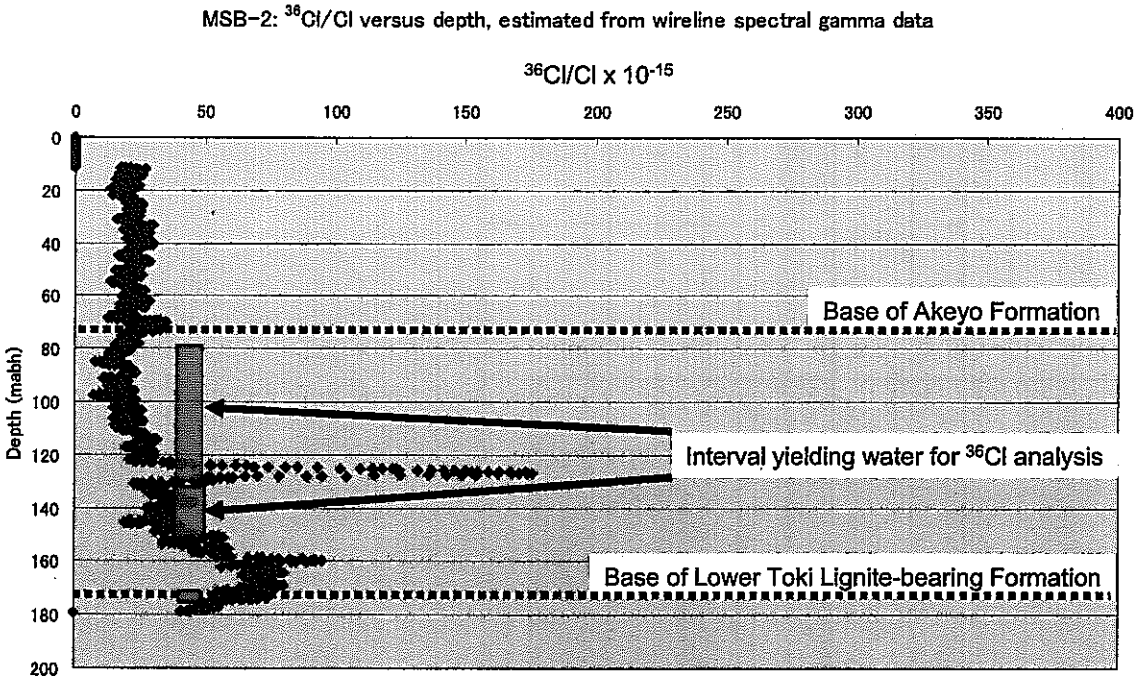

Figure 3. Theoretical equilibrium $^{36}Cl/Cl$ ratios calculated for borehole MSB-2 using spectral gamma wireline data and the approach of Lehmann and Loosli (1991). The red boxes indicate the intervals from which groundwater was sampled for ^{36}Cl analysis. Box widths indicate $\pm 2\sigma$ errors.

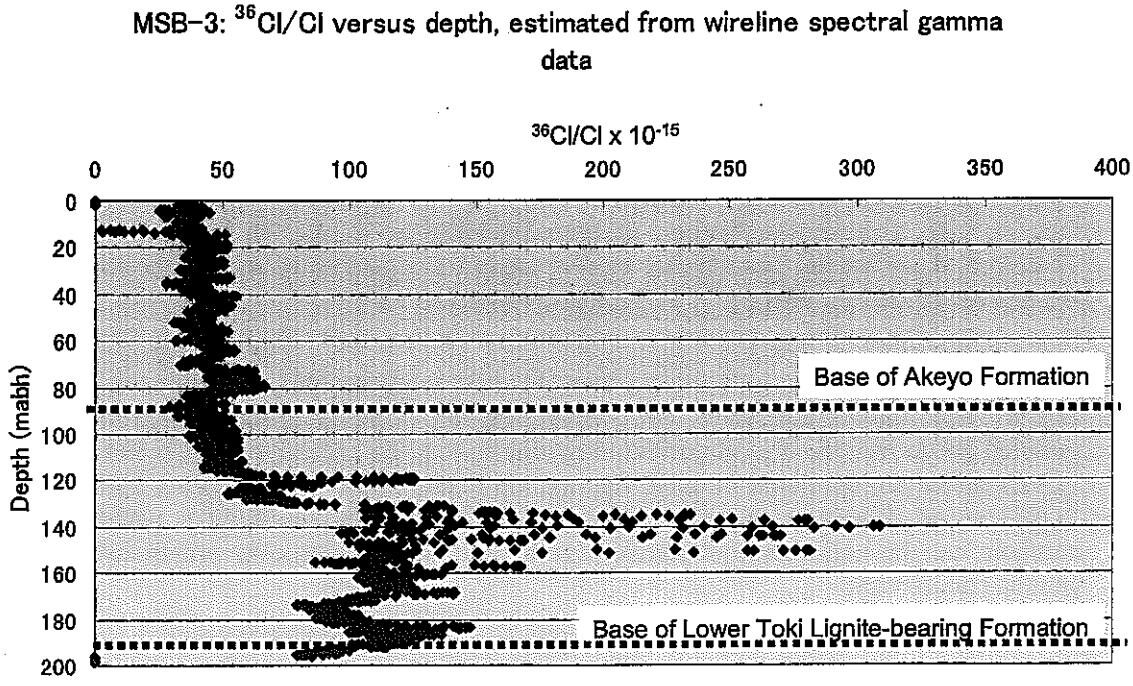

Figure 4. Theoretical equilibrium ^{36}Cl/Cl ratios calculated for borehole MSB-3 using spectral gamma wireline data and the approach of Lehmann and Loosli (1991).

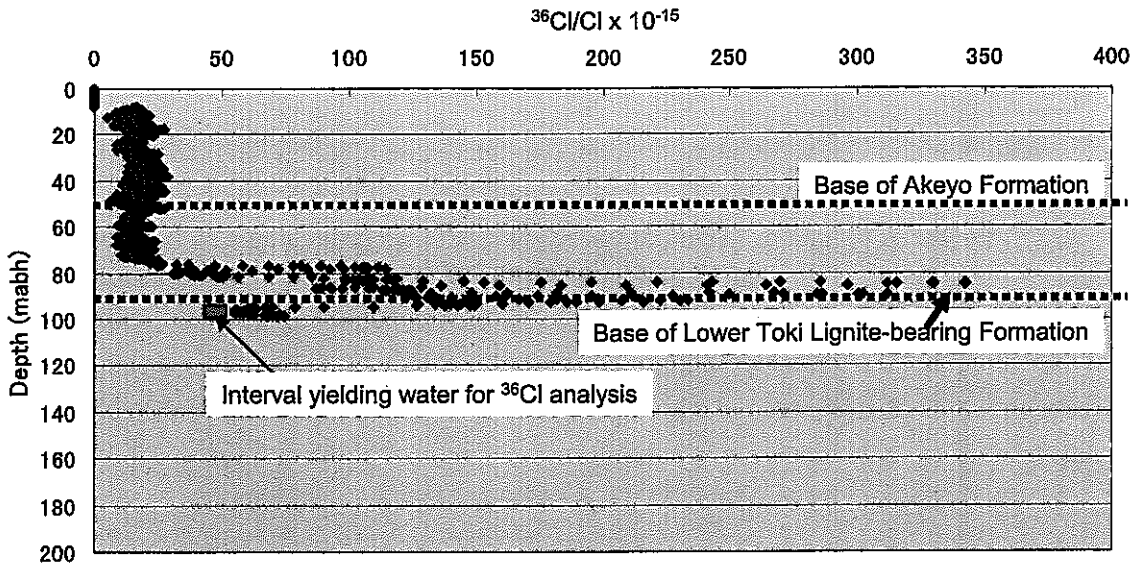

Figure 5. Theoretical equilibrium ^{36}Cl/Cl ratios calculated for borehole MSB-4 using spectral gamma wireline data and the approach of Lehmann and Loosli (1991). The red box indicates the interval from which groundwater was sampled for ^{36}Cl analysis. Box width indicates $\pm 2\sigma$ error.

For the other Tono boreholes for which there are ^{36}Cl data (MIU-4, KNA-6 and DH-12), there are no spectral gamma wireline data with which to estimate down-hole variations in *in-situ* ^{36}Cl production. However, there are natural gamma wireline data for these boreholes. While these data do not allow actual $^{36}Cl/Cl$ ratios to be calculated, they do give a general indication of the ***variability*** of U and Th concentrations. Therefore, these natural gamma data can be used to evaluate ***qualitatively***, the spatial scales over which equilibrium $^{36}Cl/Cl$ ratios are likely to vary.

The natural gamma data are plotted versus depth in the boreholes, in Figures 6, 7, 8 and 9. These figures also show, for comparison, the $^{36}Cl/Cl$ ratios measured in the sampled groundwaters. It is important to recognise that the natural gamma scales and $^{36}Cl/Cl$ scales are unrelated in these figures; the natural gamma data do not indicate $^{36}Cl/Cl$ ratios. However, the variability of the $^{36}Cl/Cl$ analyses from a particular borehole can be compared qualitatively with the length scales over which natural gamma counts vary.

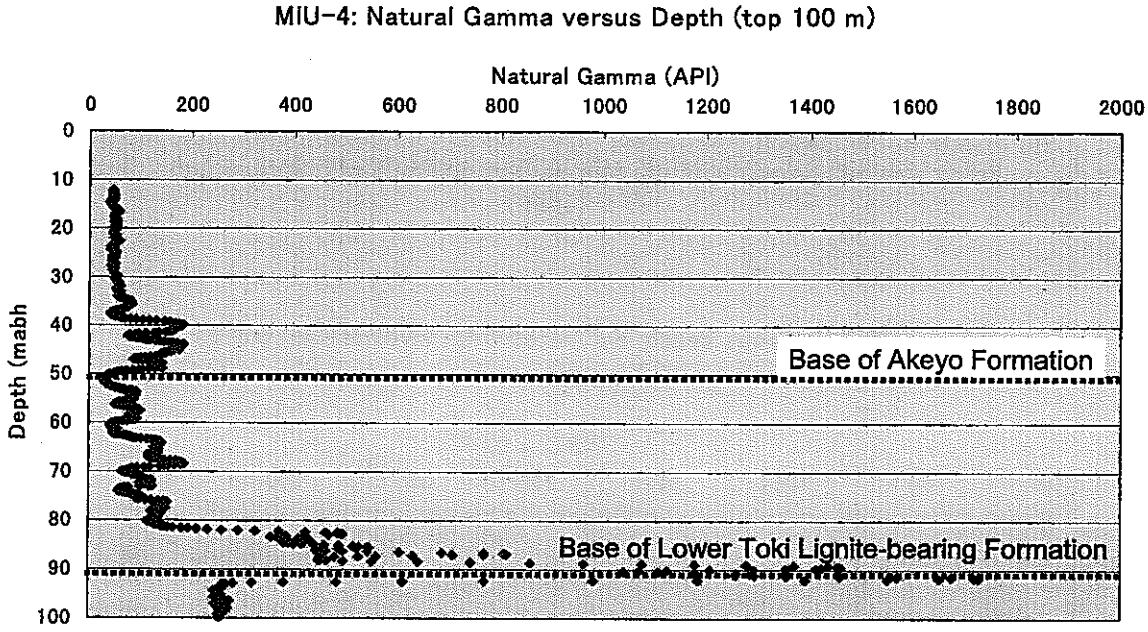

Figure 6. Variations in natural gamma data with respect to depth in the upper part of borehole MIU-4.

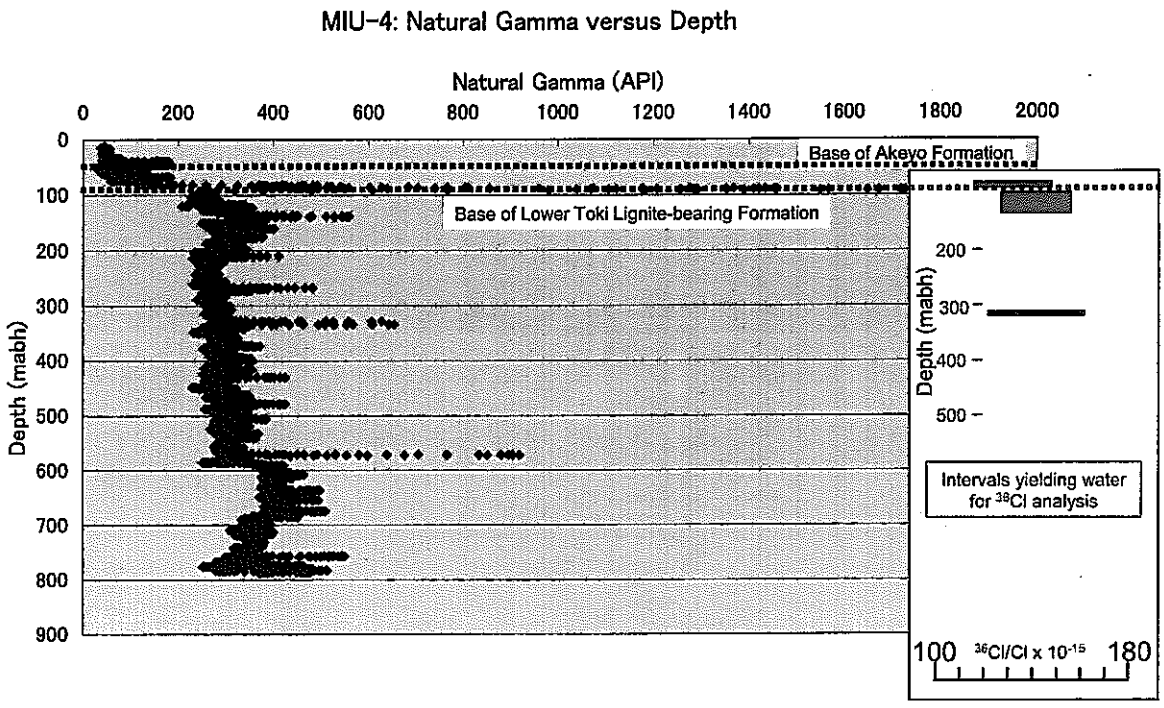

Figure 7. Variations in natural gamma data with respect to depth throughout borehole MIU-4. The inset box shows the test intervals that yielded groundwater samples for ^{36}Cl analyses, which are plotted against the red scale. The vertical scale in the inset box is the same as that in the main diagram. Box widths indicate $\pm 2\sigma$ errors.

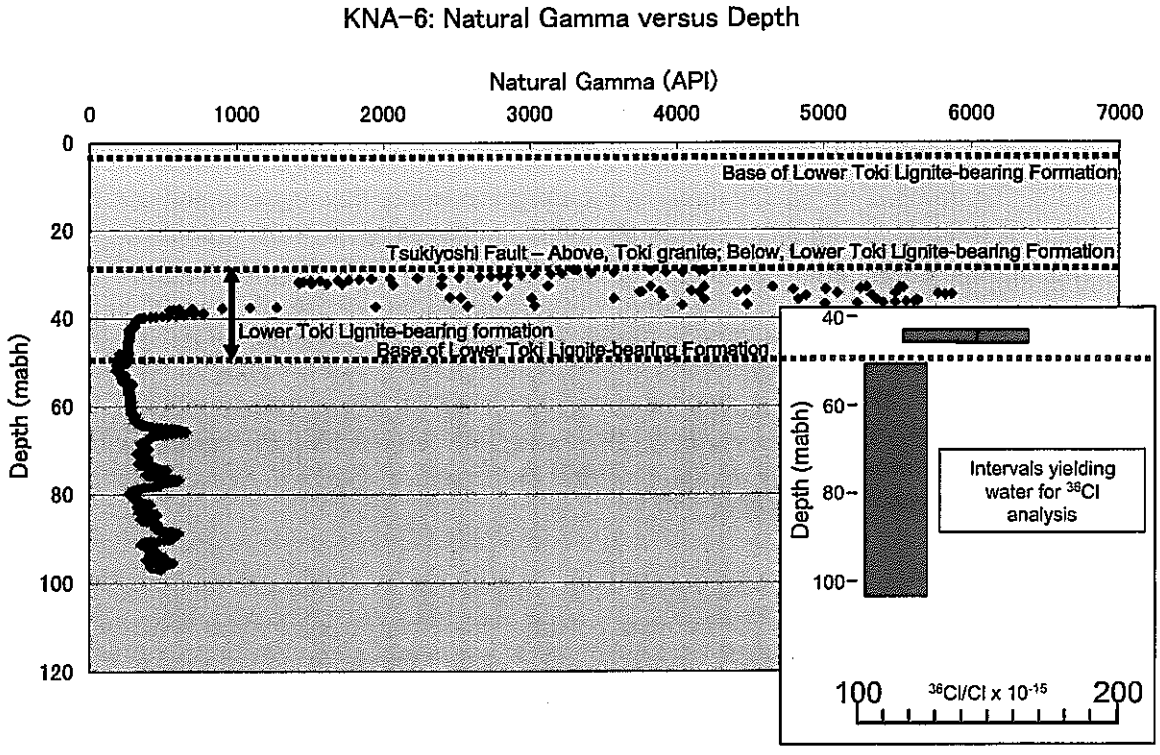

Figure 8. Variations in natural gamma data with respect to depth throughout Borehole KNA-6. The inset box shows the test intervals that yielded groundwater samples for ^{36}Cl analyses, which are plotted against the red scale. The vertical scale in the inset box is the same as that in the main diagram. Box widths indicate $\pm 2\sigma$ errors.

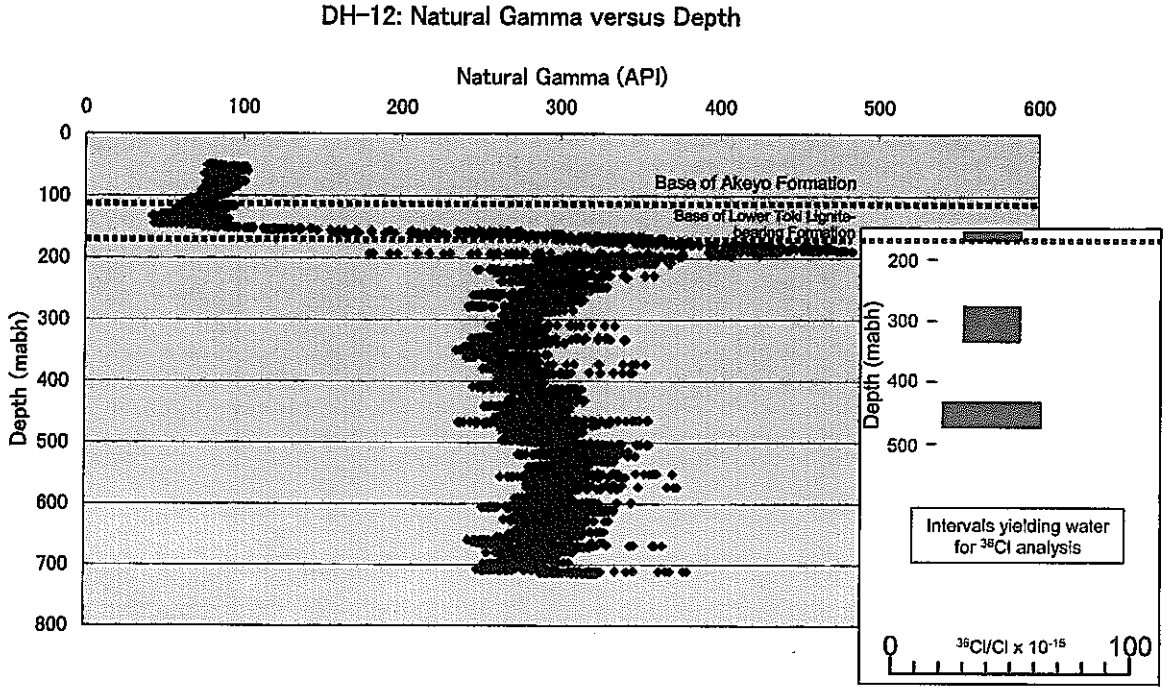

Figure 9. Variations in natural gamma data with respect to depth throughout borehole DH-12. The inset box shows the test intervals that yielded groundwater samples for ^{36}Cl analyses, which are plotted against the red scale. The vertical scale in the inset box is the same as that in the main diagram. Box widths indicate $\pm 2\sigma$ errors.

4 Discussion

4.1 Contamination

To interpret the data in terms of natural groundwater flow patterns and/or Cl residence times, it is necessary to know the source of the sampled water within the rock mass. This means either that the natural groundwater was insignificantly disturbed by anthropogenic activities such as borehole drilling and testing, or that corrections can be made for such disturbances. Where possible, care has been taken during the present work to evaluate the possible effects of such disturbances, using information supplied by JNC. However, it was outside of the scope of the project to conduct a rigorous appraisal of all possible perturbations. ***Therefore, to a large extent, the starting point for the interpretation is the assumption that the analysed waters are representative of the actual sampling localities.***

It is often more straightforward to evaluate the possible effects of contamination during sampling and analysis. The main potential source of contamination is likely to be drilling fluid. Except for KNA-6 tracer was added to the drilling fluid used to drill each borehole that gave samples for ^{36}Cl analysis. The tracer concentrations in each sample can be used to estimate the drilling fluid contamination (Table 8). Tracer concentrations for the DH-12 samples were unavailable, but it is known that these samples had <1% drilling fluid contamination.

Table 8. Summary of drilling fluid contamination levels in the analysed groundwater samples, together with an illustration of the possible significance for measured $^{36}Cl/Cl$ ratios.

Borehole	Depth range (mabh)		Tracer	Tracer Content		Contamination		Comments
	Upper	Lower		Initial	Final	% Initial Tracer	$^{36}Cl/Cl$ variation assuming drilling fluid $^{36}Cl/Cl = 400 \times 10^{-15}$	
				mg/l				
Tono Samples								
MSB-2	79.00	130.50	Na-naphthionate	10	0.17	1.7	6.8	
MSB-2	132.00	154.00	Na-naphthionate	10	0.18	1.8	7.2	
MSB-2	171.50	175.50	Uranine	0.2	0.0045	2.3	9.0	
MSB-4	95.50	99.00	Uranine	0.2	0.0007	0.3	1.4	
MIU-4	82.50	88.65	Amino-G Acid	50	0.33	0.7	2.6	
MIU-4	95.02	134.47	Eosin	3	0.03	1.0	4.0	
MIU-4	314.95	316.95	Eosin	3	0.08	2.5	10.1	
Horonobe Sample								
HDB-1	548	568.18	Na-naphthionate	10	<1.4	14.0	56.0	1.

Comments: 1. Effect on $^{36}Cl/Cl$ would be a maximum assuming $^{36}Cl/Cl$ of drilling fluid is 400×10^{-15}, but no constraint on the actual drilling fluid ratio was available.

The drilling fluids were made with fresh water from surface sources. Surface water will usually have a much larger $^{36}Cl/Cl$ ratio than deep groundwater. Therefore any drilling fluid contamination will tend to cause the sampled water to have higher $^{36}Cl/Cl$ than the undisturbed water.

Assuming that the surface waters had $^{36}Cl/Cl$ ratios similar to the Shobagawa river water (which was actually used to make the MIU-4 drilling fluid), it can be seen that contamination of the Tono samples for which there are tracer data would result in a maximum bias of $^{36}Cl/Cl$ that is comparable to or smaller than the analytical error (Table 8).

In the case of KNA-6, no information is available concerning likely drilling fluid contamination. However, this borehole was drilled several years prior to sampling for ^{36}Cl analysis and in earlier investigations, groundwater had been monitored for a prolonged period until stable Eh and pH values were obtained. The likelihood that

there was significant perturbation of the $^{36}Cl/Cl$ ratios caused by drilling fluid contamination is therefore considered to be low.

In the case of the Horonobe sample, no information about the $^{36}Cl/Cl$ of surface water was available. However, assuming that the ratio would be similar to the surface water it can be seen that the maximum contamination could be considerable. This is inconsistent with the very low $^{36}Cl/Cl$ ratio measured for the water. An implication is that the contamination is in reality much lower.

The possibility of none-drilling fluid related contamination cannot be evaluated directly, but is likely to be insignificant compared to the drilling fluid contamination. Furthermore, $^{36}Cl/Cl$ ratios are generally unaffected by sample storage.

Ideally, to evaluate the possible significance of analytical errors fully, it would be advisable to submit blind duplicate samples to the laboratory. However, as the ^{36}Cl investigations have been limited in scope and targeted at evaluating the applicability of such data, this approach was possible only in the case of the KNA-6 samples. In this case, one duplicate pair of samples, from 45.5 mabh to 46 mabh, was submitted for analysis. These samples gave $^{36}Cl/Cl$ of 151 $\pm$14 x 10^{-15} and 132 $\pm$14 x 10^{-15}, which are within the reported analytical uncertainty. These results are also significantly different from the ratios 115 $\pm$14 x 10^{-15} and 112.1 $\pm$11.8 x 10^{-15}, given by two samples from the deeper sampling interval, between 50.50 mabh and 100.00 mabh. These results suggest that at least the techniques employed are able to distinguish differences in groundwater $^{36}Cl/Cl$ ratios of around 15 x 10^{-15} to 20 x 10^{-15} in the fresh groundwaters of the northern part of the Tono area.

4.2 Variations in groundwater $^{36}Cl/Cl$ at Tono

Taking into account the contamination discussed above, the available groundwater ^{36}Cl data clearly show variations from place to place across the area (Table 4, Figure 1). The samples from MIU-4 and KNA-6 clearly gave much higher ratios than the samples from the MSB-boreholes and DH-12. It is noteworthy, however, that the ratios from the MSB-series and DH-12 boreholes are very similar.

4.3 Comparison of groundwater data and sub-surface equilibrium $^{36}Cl/Cl$

Calculations of *in-situ* production must take into account a range of uncertainties, notably caused by:

- lack of rock chemical data, especially for key trace elements such as Cl;
- uncertainties concerning rock porosities and their variations;
- poor understanding of the mechanisms by which ^{36}Cl partitions from the rock into the groundwater;
- insufficient knowledge of the mass stopping powers and cross-sections of certain elements, producing uncertainties in the calculated neutron flux.

For a given neutron flux, the $^{36}Cl/Cl$ ratio is independent of the Cl concentration in the rock or the groundwater, except possibly in limiting cases where the Cl concentration is very low relative to the K concentration. In principle, under these circumstances, ^{36}Cl production by neutron activation of ^{35}Cl could be comparable to ^{36}Cl production

by alpha-neutron reactions involving ^{39}K in the rock matrix. However, in practice, this is not the case in most rock types.

The Cl itself affects the neutron flux, which means that uncertainties in the Cl concentration of the rock and/or the water lead to uncertainties in the neutron flux and hence the calculated $^{36}Cl/Cl$ ratios. For relatively wide ranges of Cl contents in a rock, these uncertainties should be small and in many rock types can be ignored. However, it is necessary to demonstrate that this approach is justified on a case-by-case basis, as it is quite plausible that these uncertainties could become significant in some lithologies.

In the cases of the Tono rock samples, there are very few analyses of Cl. However, the available data imply that ranges of a few tens to a few hundreds of ppm are reasonable. An analysis of the Toki Granite in MIU-4 gave 230 ppm Cl, whereas a single analysis of the granite reported in Yoshida et al. (1994) indicates 22 ppm Cl. In contrast, Yoshida et al. (1994) also give Cl concentrations in the sedimentary rocks as high as 526 ppm. Over this range, the variability in $^{36}Cl/Cl$ ratios due to uncertainties in Cl is likely to be relatively small.

Possibly more serious is the lack of analyses of other key trace elements such as B, Sm and Gd. In these cases, analyses reported in the literature for similar rock types were used (Table 6).

To give a ***general*** indication of the likely significance of the uncertainties in rock composition, several estimates of *in-situ* $^{36}Cl/Cl$ were made for each sample (Table 6). From this approach it can be appreciated that the uncertainties in rock composition (excluding Cl) are likely to result in uncertainties of up to a factor of 2 in the estimates of *in-situ* $^{36}Cl/Cl$ ratios. It is, however, encouraging that the ratios estimated by the approach of Lehmann and Loosli (1991) are generally consistent with estimates based on complete whole-rock chemistry, assuming the rock contains significant Cl (c.f. estimate of $^{36}Cl/Cl$ from rock chemistry for rock containing 200 mg/l Cl and estimate from wireline data; Table 6).

Another source of uncertainty is the porosity. Clearly, the higher the porosity of a rock, the lower will be the neutron flux for a given composition. Related to this uncertainty is the composition of any pore-filling water, and especially its Cl content. In the present study, no account has been taken of these effects, with the consequence that the estimated equilibrium ratios presented here are likely to be maximum estimates.

The lower sedimentary rocks in the MSB-boreholes all have higher predicted *in-situ* equilibrium $^{36}Cl/Cl$ ratios than either the shallower sedimentary rocks or the granite (Figures 2, 3, 4 and 5). This reflects the distribution of the U-mineralisation. However, the groundwater samples gave very similar $^{36}Cl/Cl$ ratios to one another, inconsistent with them reaching local equilibrium with the *in-situ* $^{36}Cl/Cl$ production (Figures 3 and 5; Table 4). Possible interpretations are:

- The two shallower groundwater sampling intervals in MSB-2 are very wide and may sample groundwater from a range of localities with different *in-situ* $^{36}Cl/Cl$ production rates (the deepest sample from MSB-2 and the sample from MSB-4 could be close to local equilibrium in the top of the granite).

- The groundwater samples could have equilibrated with the *in-situ* $^{36}Cl/Cl$ flux in the upper granite and/or U-mineralised sedimentary rocks, and then migrated upwards.

- The natural groundwaters could be well-mixed on the scale of the borehole and the $^{36}Cl/Cl$ ratios could approach equilibrium with the mean neutron flux over this scale (c.f analyses in Table 4 with the mean equilibrium ratios in Table 7).

The $^{36}Cl/Cl$ of groundwater in MIU-4 is significantly higher than that caused by the *in-situ* neutron flux (Tables 4, 6 and 7). This implies one or more of the following:

- The Cl in the groundwater is a mixture between Cl in the recharge water (with high $^{36}Cl/Cl$) and Cl derived from the granite by water/rock interactions (with lower $^{36}Cl/Cl$).

- The Cl in the groundwater is a mixture between Cl in the recharge water (with high $^{36}Cl/Cl$) and residual Cl that originates in water having a long residence time in the granite (with lower $^{36}Cl/Cl$).

- The Cl has resided in the granite for long enough for the $^{36}Cl/Cl$ to decrease by radioactive decay, but not sufficiently long for equilibrium to be attained (see Section 4.4 for further discussion).

The wireline data suggest that the *in-situ* production in the bottom of the sedimentary rocks would be higher than the *in-situ* production in the granite. However, the groundwater sample from near the base of the sedimentary rocks gave similar results to the groundwater from the deeper granite. This may indicate that the Cl is well-mixed over the spatial scale of the samples (Figures 6, 7).

Data from borehole KNA-6 are harder to interpret in terms of Cl movement. The gamma data imply that production rates should be higher in the sedimentary rock than in the granite (Figure 8). However, the groundwater samples analysed from these two lithologies gave similar $^{36}Cl/Cl$ ratios (within error; Table 4). This may reflect the very close proximity of the sampling to the boundaries between the granite and sedimentary rocks. The ratios are similar to, or higher than the ratios given by water from MIU-4. Similar explanations to those proposed for MIU-4 (above) may be explain these values in KNA-6.

In contrast to MIU-4, the data from borehole DH-12 imply that the Cl could be in equilibrium with the *in-situ* production of ^{36}Cl in the granite (Tables 4, 6, 7). There are no rock chemical data with which to calculate equilibrium ratios for the sedimentary rocks, but the gamma log data suggest that in the lower sedimentary sequence, *in-situ* production should be higher than in the granite (Figure 9). In this case it is note-worthy that the groundwater sample from this sedimentary section gave a similar $^{36}Cl/Cl$ ratio to the two samples from the deeper granite. One possibility is that this implies upward movement of Cl from the granite into the sedimentary rocks.

There is little difference in the mean theoretical equilibrium $^{36}Cl/Cl$ ratio in the granite from boreholes DH-12 and DH-13 (Table 7). The mean value for MIU-4 is higher, but the variability is also much higher. This may be due to the relatively small number of estimates in MIU-4 and the fact that the whole-rock analyses on which they were based came from atypical features of the bulk rock (e.g. fracture walls).

There are relatively few data with which to evaluate the spatial variability of *in-situ* production of ^{36}Cl in a statistically meaningful fashion at the site scale. However, variograms can be constructed for some of the boreholes to give further insights into the length scales over which mean theoretical equilibrium $^{36}Cl/Cl$ vary (Figure 10). Here,

variograms plot a parameter representing spatial variability in $^{36}Cl/Cl$ ($\gamma(h)$) versus length scale (h; Figure 11). The former is calculated according to:

$$\gamma(h) = \frac{1}{2n(h)} \sum_{i=1}^{n(h)} \left(z_i(x) - z_i(x+h) \right)^2 \qquad \text{Equation 4.3.1}$$

where: $z_i(x)$ is the $^{36}Cl/Cl$ ratio at point x, $z_i(x + h)$ is the $^{36}Cl/Cl$ ratio at a distance h from point x, and n is the number of points at a distance h from the point x. In all the cases presented here, h is measured along each borehole.

In practice, a spacing, or 'lag' is defined, within which the points are all taken to have the same separation from the point $z_i(x)$. This approach has the effect of smoothing the variance in the data as a function of separation distance.

The variograms in Figure 11 were constructed using the code Variowin v 2.2 (Pannatier, 1996).

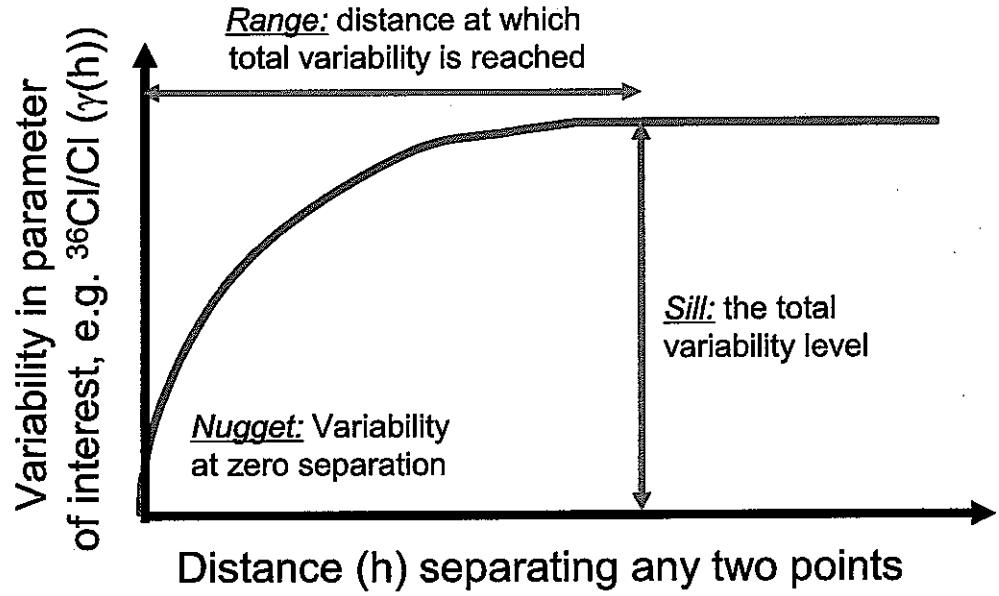

Figure 10. Schematic representation of an ***idealised*** variogram.

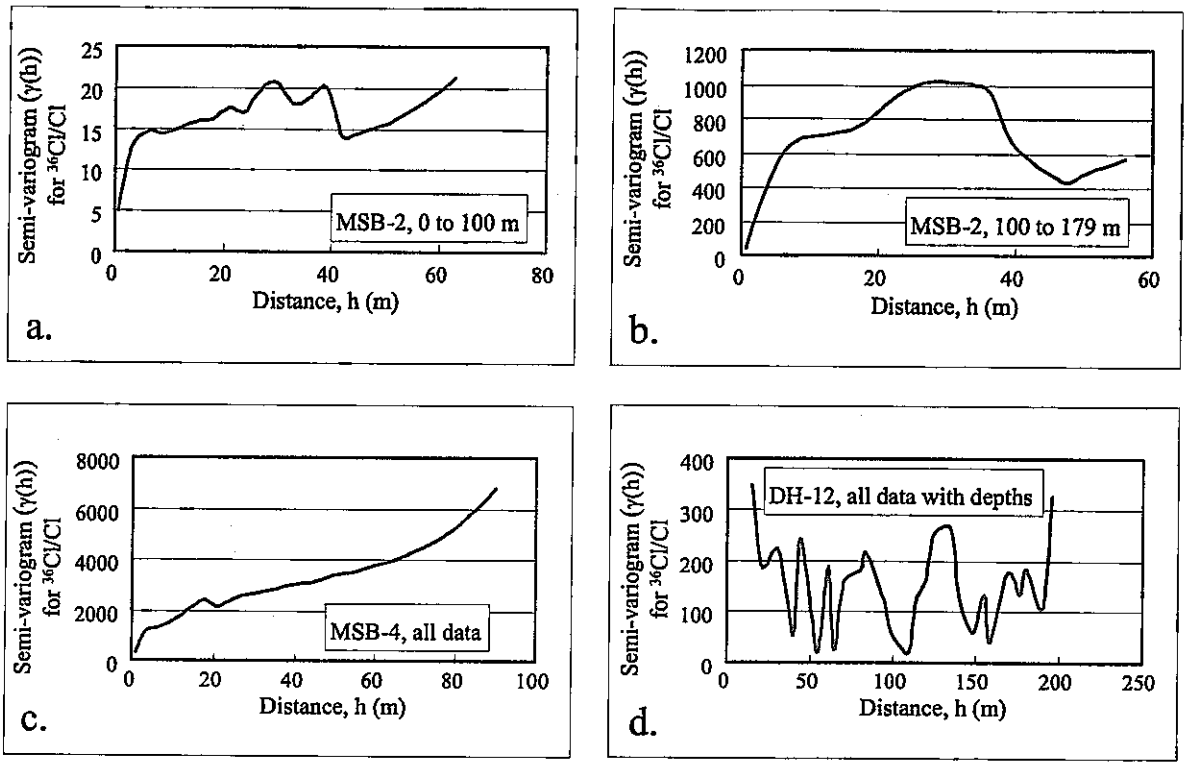

Figure 11. Variograms showing the variability in estimated ^{36}Cl/Cl in boreholes MSB-2, MSB-4 and DH-12. In a.., b. and c. the estimated ^{36}Cl/Cl ratios are based on spectral wireline data. In contrast, in d. the ratios are based on whole-rock analyses. Here, the distance, h is measured along the borehole.

The variograms in Figure 11 are all considerably different from the idealised variogram in Figure 10. Such a difference is to be expected because Figure 10 represents the simplest ideal situation in which the different samples become more different (γ(h) becomes larger) as the distance between them increases. In contrast, in the real world, the pattern of variability is usually much more complex. For example, in a sedimentary sequence in which the same type of lithology is repeated, the value of γ(h) might initially increase with distance, then decrease with distance and then increase again (Figure 12).

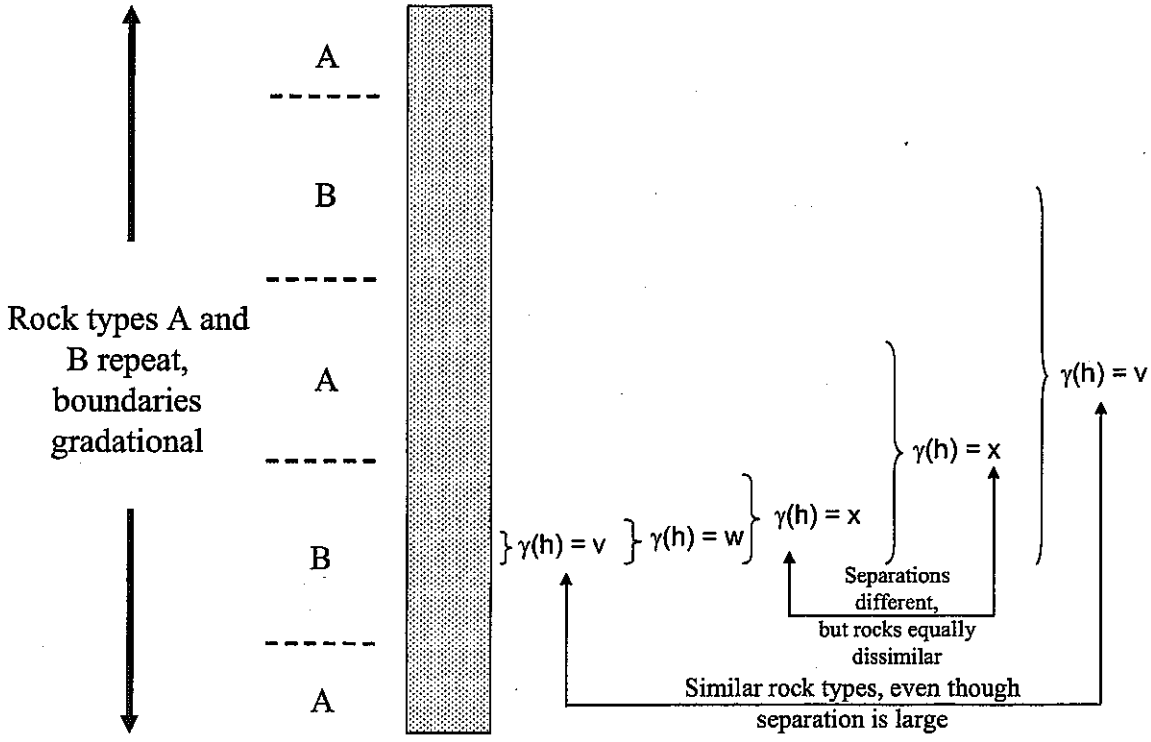

Figure 12. Schematic illustration showing how the parameter γ(h) could increase and then decrease again with increasing sample separation distance, reflecting the complex pattern of variability in the actual rock. At small spatial scales, the change in γ(h) is similar to the ideal variation in Figure 10. That is, there will be a sill at a range corresponding to half the thickness of lithology B or lithology A.

Figure 11 reflects the observation in Figures 2, 3, 4 and 5, that the *in-situ* production of ^{36}Cl in the lower part of the sedimentary rock sequence is significantly more variable than in the upper part. The variograms corresponding to the sedimentary rocks show more simple patterns than the variogram corresponding to the granite in DH-12. This is to be expected because the variability of the sedimentary rocks will be somewhat systematic, reflecting sedimentary processes (fining upwards sequences, mean bed thicknesses etc). In contrast, the variation in the granite is likely to be much less systematic on the scales of the boreholes.

Also, it may be tentatively surmised that:

- In the uppermost 120 m of the sedimentary rocks there is a range at around 10 m. Thus, spatial variability in the $^{36}Cl/Cl$ of dissolved Cl would be expected if groundwater mixed or circulated at length scales smaller than this for periods of >1.5 Ma.

- In the lower 120 m there are two apparent ranges, at around 10 m and at around 30 m. Therefore, contrasts in $^{36}Cl/Cl$ might be expected if groundwater mixed or circulated at a scale of < 10 m and/or < 30 m for > 1.5 Ma.

- The variability of *in-situ* production in the granite of DH-12 shows no correlation with respect to separation of samples, though this may reflect the small number of whole-rock samples from which the estimates were made.

- If the variability of the *in-situ* production in the granite of DH-12 is assumed to reflect adequately the actual variability, the most important observation is that $\gamma(h)$ varies (oscillates) on length scales of around 10 m to around 50 m.

An important conclusion is that several of the actual sampling intervals in the present study may be wider than the spatial scales of variability in *in-situ* ^{36}Cl production (e.g. the shallowest sampling interval in MSB-2 was 51.5 m wide). This may mean that variations in natural $^{36}Cl/Cl$ are not resolved. Ideally, groundwater should be sampled from intervals that are comparable to or shorter than the length scales outlined above.

4.4 Model residence times

There is insufficient information with which to calculate reliable residence times for the Cl in the various rock formations. However, illustrative residence times have been calculated based on various simplifying assumptions (Table 9). To do this, the following equation was employed:

$$t = \frac{-1}{\lambda_{^{36}Cl}} \ln\left(\frac{R - R_{se}}{R_0 - R_{se}}\right) \qquad \text{Equation 4.4.1}$$

where: t = time in years
λ_{36Cl} = decay constant of ^{36}Cl (2.30×10^{-6} a^{-1})
R = measured $^{36}Cl/Cl$ ratio;
R_0 = initial ratio on entry to the rock formation;
R_{se} = secular equilibrium ratio that would be produced by *in situ* neutron flux.

Several hundred thousand years would possibly be needed for the Cl in recharge water to achieve the observed $^{36}Cl/Cl$ ratios in the deep groundwater samples from MIU-4. These times are far in excess of calculated groundwater travel times based on hydrogeological data or other isotopic indicators, such as ^{14}C. This comparison indirectly supports the alternative hypothesis that the Cl in the groundwater from MIU-4 is a mixture between Cl derived from recharge and Cl derived from water/rock interaction or a component of 'older' water that has resided in the granite for a long time.

It is possible that the relatively high $^{36}Cl/Cl$ ratios in borehole KNA-6 could have a similar origin to those in the MIU-4 samples. This would be consistent with the ^{14}C data from groundwater sampled near the base of the sedimentary rocks around Tono mine. However a possible complication is that KNA-6 is located near to the centre of the Tsukiyoshi ore deposit and *in-situ* production rates might be expected to be much higher than in the granite of MIU-4. In KNA-6 much less time might be needed to produce the *in-situ* equilibrium rates.

The residence time needed to produce a detectable change in groundwater is strongly dependent upon the spatial scale over which the Cl can mix (Figure 11). In this case, if water moved into the deeper sedimentary rock containing the highest U and Th concentrations and stayed there (did not move more than 1 m or so from 127 m depth), then < 10,000 years would be needed to produce a detectable variation in $^{36}Cl/Cl$ ratio. In contrast, if the water was able to circulate and homogenise within the lower sedimentary rocks, between 120 m and the top of the granite, a time of several ten's of thousand years to more than 100,000 years would be needed (Table 9, Figure 13).

Table 9. Model residence times, intended to illustrate the time scales required for $^{36}Cl/Cl$ variations to occur *in-situ*.

	$^{36}Cl/Cl \times 10^{15}$				
Time estimated	**Inflow $^{36}Cl/Cl$**	**Groundwater $^{36}Cl/Cl$**	**Equilibrium $^{36}Cl/Cl$**	**Model Time**	**Comments**
	x 10^{-15}	**x 10^{-15}**	**x 10^{-15}**	**years**	
Minimum time for Shobagawa river water to acquire the $^{36}Cl/Cl$ of the Toki Granite groundwater, assuming well mixed in the granite.	409	147	54	583278	Inflow $^{36}Cl/Cl$: Shobagawa river water ratio Final groundwater ratio: smallest groundwater ratio plus 1σ taken as the final groundwater ratio Equilibrium ratio: mean calculated from wireline data
Minimum time for Shobagawa river water to acquire the $^{36}Cl/Cl$ of the Toki Granite groundwater, assuming water flows through fractures lined by low U- and Th-minerals.	409	159	12	431356	Inflow $^{36}Cl/Cl$: Shobagawa river water ratio Final groundwater ratio: largest groundwater ratio plus1σ Equilibrium ratio: mean calculated from wireline data minus 1σ.
Minimum time for MSB-2 water to reside in the sedimentary rocks above 120 m depth to decrease $^{36}Cl/Cl$ by > 1 σ error.	44	41	17	48920	Inflow $^{36}Cl/Cl$: largest groundwater ratio Final groundwater ratio: largest reported groundwater ratio minus 1σ Equilibrium ratio: mean ratio calculated from wireline data in the interval above 120 m minus 1σ
Minimum time for MSB-2 water to reside in the sedimentary rocks below 120 m depth to increase $^{36}Cl/Cl$ by > 1 σ error.	44	47	82	35176	Inflow $^{36}Cl/Cl$: initial groundwater ratio Final groundwater ratio: largest reported groundwater ratio plus 1σ Equilibrium ratio: mean ratio calculated from wireline data in the interval below 120 m plus 1σ

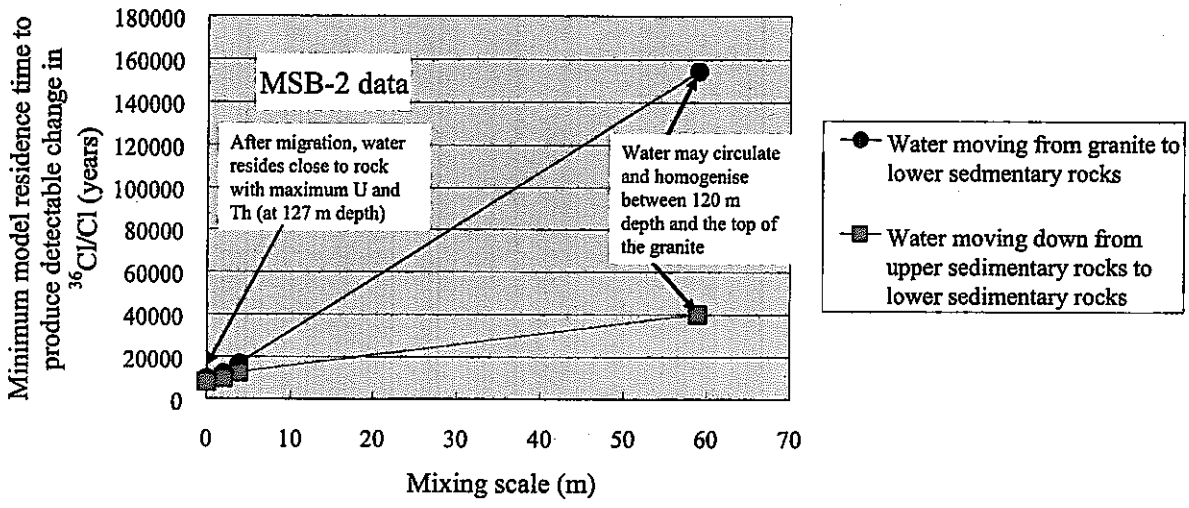

Figure 13. Illustration of the possible effect of mixing at different length scales on the residence times required to produce detectable variations in the ^{36}Cl/Cl ratios of dissolved Cl. The water initially contains Cl equilibrated with *in-situ* ^{36}Cl production either in the sedimentary rocks shallower than 120 m (downwards flowing case), or the granite (upwards flowing case).

5 Comparison with data from Horonobe HDB-1

The sample from borehole HDB-1 at Horonobe gave ^{36}Cl/Cl much lower than any sample from the Tono area (Tables 4 and 5). This reflects the chemistry of the host rocks and possibly also the origin of the Cl. Compared to the rocks at Tono the Wakkanai Formation would have lower *in-situ* equilibrium ^{36}Cl/Cl (Table 6). Additionally, a possible origin of the Cl at Horonobe is palaeo-seawater. Seawater would have had an initial ratio that was effectively zero. However, it is stressed that there is only one Horonobe groundwater sample and no corresponding rock analyses. Much more data are needed to reach firm conclusions about the origin and residence time of the Cl at Horonobe.

6 Conclusions

Several key conclusions can be drawn:

- The results of this study suggest that, if ^{36}Cl data can be obtained for groundwaters at spatial scales comparable to, or smaller than, the variability in *in-situ* ^{36}Cl production in the host rock, they could potentially be useful for interpreting groundwater origins and flow patterns.

- In the northern part of the study area, which is dominated by fresh groundwaters to sampled depths of 1000 m, ^{36}Cl data may help to indicate the presence of relatively recently recharged meteoric water.

- The ^{36}Cl/Cl ratios in the groundwaters from MIU-4 (and possibly also those from KNA-6) may reflect mixing between Cl derived from recharge and Cl derived from the rock during water/rock interactions, or from mixing with a component of 'older' groundwater.

- The $^{36}Cl/Cl$ ratios of groundwater in the granite from DH-12 could reflect equilibration with *in-situ* ^{36}Cl production, implying a residence time in the granite in excess of 1.5 Ma.

- The granite in different parts of the area may have similar overall mean *in-situ* ^{36}Cl production at the scale of 100's to 1000's of m. Therefore, groundwater circulating over such length scales in different areas would acquire similar equilibrium $^{36}Cl/Cl$ ratios after > c. 1.5 Ma. The fact that the Cl in DH-12 could have resided in the granite for > 1.5 Ma does not mean that it necessarily resided in the vicinity of DH-12 for > 1.5 Ma.

- The wireline data from the MSB-boreholes suggest that there could be significant contrasts in *in-situ* ^{36}Cl production between different locations. This suggests the possibility that is might be possible to obtain groundwater ^{36}Cl data from these boreholes that may be useful for evaluating groundwater flow.

- In MSB-2, the groundwater Cl appears to be well-mixed over the sampled interval, between 79 m to 176 m depth.

- In this borehole, the groundwater Cl cannot have equilibrated with the *in-situ* ^{36}Cl production above 120 m depth. Instead, the Cl originated at greater depths.

- If water containing Cl that had equilibrated with the mean in-situ neutron flux in the granite moved upwards into the lower sedimentary rocks in MSB-2, the water would subsequently need to remain stationary for at least several tens of thousands of years to produce observable spatial variations in $^{36}Cl/Cl$ ratios.

- Some of the groundwater sampling intervals are wide compared to the spatial scale of variability in in-situ production and therefore variations in natural $^{36}Cl/Cl$ in the dissolved Cl may not be resolved.

- Future sampling should focus on obtaining groundwater samples from intervals much smaller than the spatial scale over which in-situ ^{36}Cl production varies. A possible complimentary approach to sampling groundwaters would be to analyse ^{36}Cl in leachates and squeezed porewaters obtained from core samples.

7 References

Andrews, J.N., Edmunds, W.M., Smedley, P.L., Fontes, J-Ch., Fifield, L.K. and Allan, G.L. 1994. Chlorine-36 in groundwater as a palaeoclimatic indicator: the East Midlands Triassic sandstone aquifer (U.K.). Earth and Planetary Science Letters, 122, 159-171.

Andrews J. N., Davis S. N., Fabryka-Martin J., Fontes J.-C., Lehmann B. E., Loosli H. H., Michelot J.-L., Moser H., Smith B., and Wolf M. 1989. The in-situ production of radioisotopes in rock matrices with particular reference to the Stripa granite. Geochimica et Cosmochimica Acta 53, 1803-1815.

Andrews J. N., Fontes J. C., Michelot J. L., and Elmore D. 1986. In-situ neutron flux, ^{36}Cl production and groundwater evolution in crystalline rocks at Stripa, Sweden. Earth and Planetary Science Letters 77, 49-58.

Elmore D. and others. 1993. The Perdue rare isotope measurement laboratory. Perdue University, Indiana.

Lehmann, B.E. and Loosli, H.H. 1991. Isotopes formed by underground production. In: Pearson, F.J., Balderer, W., Looslie, H.H., Lehmann, B.E., Matter, A., Peters, T., Schassmann, H. and Gautschi, A. (eds), Applied isotope hydrogeology: a case study in northern Switzerland. Studies in Environmental Science, 43, Elsevier, 239-265.

Pannatier, Y. 1996. VARIOWIN: Software for Spatial Data Analysis in 2D.
Springer Verlag, Berlin. 91p.

Phillips, F.M. Bentley, H.W. and Elmore, D. 1986. Chlorine-36 dating of old groundwater in sedimentary basins. In: Hydrogeology of sedimentary basins: application to exploration and exploitation. Proceedings of the 3rd Canadian/American conference on hydrogeology, Banff, Canada. Alberta Research Council; National Water Wells Association. 143-150.

Yoshida, H., Seo, T., Nohara, T., Ota, K., Hama, K., Kodama, K. And Iwatsuki, T. 1994 Data compilation of geoscientific studies of Tono uranium deposits, central Japan. PNC Report PNC TN7410 94-015.

Appendix A: Rock compositions used in the calculation of in-situ ^{36}Cl production

Well No.	Depth	SiO_2	TiO_2	Al_2O_3	Fe_2O_3	FeO	MnO	MgO	CaO	Na_2O	K_2O	P_2O_5	Total	H_2O^+	Th	U	CO_2	Cl	F	Cr	Co	Ni	Sm	Gd	Be	N	Li	B	Comments
	mbGL	Wt%[1]	Wt%	Wt%	Wt%	Wt%	Wt%	Wt%	Wt%	Wt%	Wt%	Wt%	Wt%	Wt%	ppm	ppm	Wt%	ppm	ppm	ppm	ppm	ppm	ppm	ppm	ppm	ppm	ppm	ppm	
DH-12	181.15	73.83	0.20	12.87	2.14	1.37	0.05	0.29	0.97	2.89	4.74	0.06	98.83	0.64	14.9	7.1	0.001	1	1.E-06	1.E-06	1.E-06	1.E-06	1.E-06	1.E-06	1.E-06	1.E-06	1.E-06	1.E-06	CO_2 at detection limit, negligible Cr, Co, Ni, Sm, Gd, Be, N, Li, B
DH-12	272.60	72.50	0.20	13.46	1.86	1.39	0.06	0.24	1.46	3.32	5.09	0.04	98.48	0.17	21.6	3.6	0.001	1	1.E-06	1.E-06	1.E-06	1.E-06	1.E-06	1.E-06	1.E-06	1.E-06	1.E-06	1.E-06	CO_2 at detection limit, negligible Cr, Co, Ni, Sm, Gd, Be, N, Li, B
DH-12	289.48	N.R.	N.R.	N.R.	N.R.	N.R.	N.R.	N.R.	N.R.	N.R.	N.R.	N.R.	N.R.	N.R.	8.9	2.3	0.001	1	1.E-06	1.E-06	1.E-06	1.E-06	1.E-06	1.E-06	1.E-06	1.E-06	1.E-06	1.E-06	CO_2 at detection limit, negligible Cr, Co, Ni, Sm, Gd, Be, N, Li, B
DH-12	301.18	75.46	0.21	11.91	2.27	1.57	0.07	0.36	1.54	3.03	3.75	0.06	98.98	0.13	18.6	3.4	0.001	1	1.E-06	1.E-06	1.E-06	1.E-06	1.E-06	1.E-06	1.E-06	1.E-06	1.E-06	1.E-06	CO_2 at detection limit, negligible Cr, Co, Ni, Sm, Gd, Be, N, Li, B
DH-12	314.45	N.R.	N.R.	N.R.	N.R.	N.R.	N.R.	N.R.	N.R.	N.R.	N.R.	N.R.	N.R.	N.R.	12.1	2.0	0.001	1	1.E-06	1.E-06	1.E-06	1.E-06	1.E-06	1.E-06	1.E-06	1.E-06	1.E-06	1.E-06	CO_2 at detection limit, negligible Cr, Co, Ni, Sm, Gd, Be, N, Li, B
DH-12	330.40	74.75	0.20	12.53	2.05	1.48	0.06	0.23	1.49	3.04	4.08	0.07	98.71	0.12	16.0	2.2	0.001	1	1.E-06	1.E-06	1.E-06	1.E-06	1.E-06	1.E-06	1.E-06	1.E-06	1.E-06	1.E-06	CO_2 at detection limit, negligible Cr, Co, Ni, Sm, Gd, Be, N, Li, B
DH-12	348.65	N.R.	N.R.	N.R.	N.R.	N.R.	N.R.	N.R.	N.R.	N.R.	N.R.	N.R.	N.R.	N.R.	8.5	1.5	0.001	1	1.E-06	1.E-06	1.E-06	1.E-06	1.E-06	1.E-06	1.E-06	1.E-06	1.E-06	1.E-06	CO_2 at detection limit, negligible Cr, Co, Ni, Sm, Gd, Be, N, Li, B
DH-12	369.95	73.51	0.22	12.93	2.32	1.18	0.08	0.31	1.66	3.27	3.99	0.16	98.80	0.23	15.0	4.2	0.001	1	1.E-06	1.E-06	1.E-06	1.E-06	1.E-06	1.E-06	1.E-06	1.E-06	1.E-06	1.E-06	CO_2 at detection limit, negligible Cr, Co, Ni, Sm, Gd, Be, N, Li, B
DH-12	420.15	73.67	0.20	13.36	2.16	1.81	0.07	0.27	1.51	3.43	4.29	0.05	99.35	0.21	27.7	5.5	0.001	1	1.E-06	1.E-06	1.E-06	1.E-06	1.E-06	1.E-06	1.E-06	1.E-06	1.E-06	1.E-06	CO_2 at detection limit, negligible Cr, Co, Ni, Sm, Gd, Be, N, Li, B
DH-12	435.80	71.11	0.22	13.67	2.06	1.48	0.08	0.21	1.61	3.67	5.04	0.07	98.08	0.26	16.3	3.9	0.001	1	1.E-06	1.E-06	1.E-06	1.E-06	1.E-06	1.E-06	1.E-06	1.E-06	1.E-06	1.E-06	CO_2 at detection limit, negligible Cr, Co, Ni, Sm, Gd, Be, N, Li, B
DH-12	450.25	74.38	0.18	12.96	1.83	1.24	0.06	0.19	1.38	3.04	4.60	0.06	98.93	0.16	15.0	2.8	0.001	1	1.E-06	1.E-06	1.E-06	1.E-06	1.E-06	1.E-06	1.E-06	1.E-06	1.E-06	1.E-06	CO_2 at detection limit, negligible Cr, Co, Ni, Sm, Gd, Be, N, Li, B
DH-12	465.25	72.04	0.20	13.84	2.05	1.48	0.08	0.31	1.37	3.27	5.11	0.05	99.04	0.52	12.2	8.9	0.001	1	1.E-06	1.E-06	1.E-06	1.E-06	1.E-06	1.E-06	1.E-06	1.E-06	1.E-06	1.E-06	CO_2 at detection limit, negligible Cr, Co, Ni, Sm, Gd, Be, N, Li, B
DH-12	479.85	75.01	0.19	12.47	1.94	1.68	0.07	0.25	1.35	3.14	4.33	0.04	99.07	0.16	17.2	2.5	0.001	1	1.E-06	1.E-06	1.E-06	1.E-06	1.E-06	1.E-06	1.E-06	1.E-06	1.E-06	1.E-06	CO_2 at detection limit, negligible Cr, Co, Ni, Sm, Gd, Be, N, Li, B
DH-12	181.15	73.83	0.20	12.87	2.14	1.37	0.05	0.29	0.97	2.89	4.74	0.06	98.83	0.64	14.9	7.1	0.001	200	1.E-06	1.E-06	1.E-06	1.E-06	1.E-06	1.E-06	1.E-06	1.E-06	1.E-06	1.E-06	CO_2 at detection limit, negligible Cr, Co, Ni, Sm, Gd, Be, N, Li, B
DH-12	272.60	72.50	0.20	13.46	1.86	1.39	0.06	0.24	1.46	3.32	5.09	0.04	98.48	0.17	21.6	3.6	0.001	200	1.E-06	1.E-06	1.E-06	1.E-06	1.E-06	1.E-06	1.E-06	1.E-06	1.E-06	1.E-06	CO_2 at detection limit, negligible Cr, Co, Ni, Sm, Gd, Be, N, Li, B
DH-12	289.48	N.R.	N.R.	N.R.	N.R.	N.R.	N.R.	N.R.	N.R.	N.R.	N.R.	N.R.	N.R.	N.R.	8.9	2.3	0.001	200	1.E-06	1.E-06	1.E-06	1.E-06	1.E-06	1.E-06	1.E-06	1.E-06	1.E-06	1.E-06	CO_2 at detection limit, negligible Cr, Co, Ni, Sm, Gd, Be, N, Li, B
DH-12	301.18	75.46	0.21	11.91	2.27	1.57	0.07	0.36	1.54	3.03	3.75	0.06	98.98	0.13	18.6	3.4	0.001	200	1.E-06	1.E-06	1.E-06	1.E-06	1.E-06	1.E-06	1.E-06	1.E-06	1.E-06	1.E-06	CO_2 at detection limit, negligible Cr, Co, Ni, Sm, Gd, Be, N, Li, B
DH-12	314.45	N.R.	N.R.	N.R.	N.R.	N.R.	N.R.	N.R.	N.R.	N.R.	N.R.	N.R.	N.R.	N.R.	12.1	2.0	0.001	200	1.E-06	1.E-06	1.E-06	1.E-06	1.E-06	1.E-06	1.E-06	1.E-06	1.E-06	1.E-06	CO_2 at detection limit, negligible Cr, Co, Ni, Sm, Gd, Be, N, Li, B
DH-12	330.40	74.75	0.20	12.53	2.05	1.48	0.06	0.23	1.49	3.04	4.08	0.07	98.71	0.12	16.0	2.2	0.001	200	1.E-06	1.E-06	1.E-06	1.E-06	1.E-06	1.E-06	1.E-06	1.E-06	1.E-06	1.E-06	CO_2 at detection limit, negligible Cr, Co, Ni, Sm, Gd, Be, N, Li, B
DH-12	348.65	N.R.	N.R.	N.R.	N.R.	N.R.	N.R.	N.R.	N.R.	N.R.	N.R.	N.R.	N.R.	N.R.	8.5	1.5	0.001	200	1.E-06	1.E-06	1.E-06	1.E-06	1.E-06	1.E-06	1.E-06	1.E-06	1.E-06	1.E-06	CO_2 at detection limit, negligible Cr, Co, Ni, Sm, Gd, Be, N, Li, B
DH-12	369.95	73.51	0.22	12.93	2.32	1.18	0.08	0.31	1.66	3.27	3.99	0.16	98.80	0.23	15.0	4.2	0.001	200	1.E-06	1.E-06	1.E-06	1.E-06	1.E-06	1.E-06	1.E-06	1.E-06	1.E-06	1.E-06	CO_2 at detection limit, negligible Cr, Co, Ni, Sm, Gd, Be, N, Li, B
DH-12	420.15	73.67	0.20	13.36	2.16	1.81	0.07	0.27	1.51	3.43	4.29	0.05	99.35	0.21	27.7	5.5	0.001	200	1.E-06	1.E-06	1.E-06	1.E-06	1.E-06	1.E-06	1.E-06	1.E-06	1.E-06	1.E-06	CO_2 at detection limit, negligible Cr, Co, Ni, Sm, Gd, Be, N, Li, B
DH-12	435.80	71.11	0.22	13.67	2.06	1.48	0.08	0.21	1.61	3.67	5.04	0.07	98.08	0.26	16.3	3.9	0.001	200	1.E-06	1.E-06	1.E-06	1.E-06	1.E-06	1.E-06	1.E-06	1.E-06	1.E-06	1.E-06	CO_2 at detection limit, negligible Cr, Co, Ni, Sm, Gd, Be, N, Li, B
DH-12	450.25	74.38	0.18	12.96	1.83	1.24	0.06	0.19	1.38	3.04	4.60	0.06	98.93	0.16	15.0	2.8	0.001	200	1.E-06	1.E-06	1.E-06	1.E-06	1.E-06	1.E-06	1.E-06	1.E-06	1.E-06	1.E-06	CO_2 at detection limit, negligible Cr, Co, Ni, Sm, Gd, Be, N, Li, B
DH-12	465.25	72.04	0.20	13.84	2.05	1.48	0.08	0.31	1.37	3.27	5.11	0.05	99.04	0.52	12.2	8.9	0.001	200	1.E-06	1.E-06	1.E-06	1.E-06	1.E-06	1.E-06	1.E-06	1.E-06	1.E-06	1.E-06	CO_2 at detection limit, negligible Cr, Co, Ni, Sm, Gd, Be, N, Li, B
DH-12	479.85	75.01	0.19	12.47	1.94	1.68	0.07	0.25	1.35	3.14	4.33	0.04	99.07	0.16	17.2	2.5	0.001	200	1.E-06	1.E-06	1.E-06	1.E-06	1.E-06	1.E-06	1.E-06	1.E-06	1.E-06	1.E-06	CO_2 at detection limit, negligible Cr, Co, Ni, Sm, Gd, Be, N, Li, B
DH-12	181.15	73.83	0.20	12.87	2.14	1.37	0.05	0.29	0.97	2.89	4.74	0.06	98.83	0.64	14.9	7.1	0.001	1	440	1.7	0.7	8	11.4	12.9	5.5	20	11	4	CO_2 at detection limit, Cr, Co, Ni, Sm, Gd, Be, N, Li, B: Stripa Granite (Andrews et al. 1989)
DH-12	272.60	72.50	0.20	13.46	1.86	1.39	0.06	0.24	1.46	3.32	5.09	0.04	98.48	0.17	21.6	3.6	0.001	1	440	1.7	0.7	8	11.4	12.9	5.5	20	11	4	CO_2 at detection limit, Cr, Co, Ni, Sm, Gd, Be, N, Li, B: Stripa Granite (Andrews et al. 1989)
DH-12	289.48	N.R.	N.R.	N.R.	N.R.	N.R.	N.R.	N.R.	N.R.	N.R.	N.R.	N.R.	N.R.	N.R.	8.9	2.3	0.001	1	440	1.7	0.7	8	11.4	12.9	5.5	20	11	4	CO_2 at detection limit, Cr, Co, Ni, Sm, Gd, Be, N, Li, B: Stripa Granite (Andrews et al. 1989)
DH-12	301.18	75.46	0.21	11.91	2.27	1.57	0.07	0.36	1.54	3.03	3.75	0.06	98.98	0.13	18.6	3.4	0.001	1	440	1.7	0.7	8	11.4	12.9	5.5	20	11	4	CO_2 at detection limit, Cr, Co, Ni, Sm, Gd, Be, N, Li, B: Stripa Granite (Andrews et al. 1989)
DH-12	314.45	N.R.	N.R.	N.R.	N.R.	N.R.	N.R.	N.R.	N.R.	N.R.	N.R.	N.R.	N.R.	N.R.	12.1	2.0	0.001	1	440	1.7	0.7	8	11.4	12.9	5.5	20	11	4	CO_2 at detection limit, Cr, Co, Ni, Sm, Gd, Be, N, Li, B: Stripa Granite (Andrews et al. 1989)
DH-12	330.40	74.75	0.20	12.53	2.05	1.48	0.06	0.23	1.49	3.04	4.08	0.07	98.71	0.12	16.0	2.2	0.001	1	440	1.7	0.7	8	11.4	12.9	5.5	20	11	4	CO_2 at detection limit, Cr, Co, Ni, Sm, Gd, Be, N, Li, B: Stripa Granite (Andrews et al. 1989)
DH-12	348.65	N.R.	N.R.	N.R.	N.R.	N.R.	N.R.	N.R.	N.R.	N.R.	N.R.	N.R.	N.R.	N.R.	8.5	1.5	0.001	1	440	1.7	0.7	8	11.4	12.9	5.5	20	11	4	CO_2 at detection limit, Cr, Co, Ni, Sm, Gd, Be, N, Li, B: Stripa Granite (Andrews et al. 1989)
DH-12	369.95	73.51	0.22	12.93	2.32	1.18	0.08	0.31	1.66	3.27	3.99	0.16	98.80	0.23	15.0	4.2	0.001	1	440	1.7	0.7	8	11.4	12.9	5.5	20	11	4	CO_2 at detection limit, Cr, Co, Ni, Sm, Gd, Be, N, Li, B: Stripa Granite (Andrews et al. 1989)
DH-12	420.15	73.67	0.20	13.36	2.16	1.81	0.07	0.27	1.51	3.43	4.29	0.05	99.35	0.21	27.7	5.5	0.001	1	440	1.7	0.7	8	11.4	12.9	5.5	20	11	4	CO_2 at detection limit, Cr, Co, Ni, Sm, Gd, Be, N, Li, B: Stripa Granite (Andrews et al. 1989)
DH-12	435.80	71.11	0.22	13.67	2.06	1.48	0.08	0.21	1.61	3.67	5.04	0.07	98.08	0.26	16.3	3.9	0.001	1	440	1.7	0.7	8	11.4	12.9	5.5	20	11	4	CO_2 at detection limit, Cr, Co, Ni, Sm, Gd, Be, N, Li, B: Stripa Granite (Andrews et al. 1989)
DH-12	450.25	74.38	0.18	12.96	1.83	1.24	0.06	0.19	1.38	3.04	4.60	0.06	98.93	0.16	15.0	2.8	0.001	1	440	1.7	0.7	8	11.4	12.9	5.5	20	11	4	CO_2 at detection limit, Cr, Co, Ni, Sm, Gd, Be, N, Li, B: Stripa Granite (Andrews et al. 1989)
DH-12	465.25	72.04	0.20	13.84	2.05	1.48	0.08	0.31	1.37	3.27	5.11	0.05	99.04	0.52	12.2	8.9	0.001	1	440	1.7	0.7	8	11.4	12.9	5.5	20	11	4	CO_2 at detection limit, Cr, Co, Ni, Sm, Gd, Be, N, Li, B: Stripa Granite (Andrews et al. 1989)
DH-12	479.85	75.01	0.19	12.47	1.94	1.68	0.07	0.25	1.35	3.14	4.33	0.04	99.07	0.16	17.2	2.5	0.001	1	440	1.7	0.7	8	11.4	12.9	5.5	20	11	4	CO_2 at detection limit, Cr, Co, Ni, Sm, Gd, Be, N, Li, B: Stripa Granite (Andrews et al. 1989)
DH-12	181.15	73.83	0.20	12.87	2.14	1.37	0.05	0.29	0.97	2.89	4.74	0.06	98.83	0.64	14.9	7.1	0.001	200	440	1.7	0.7	8	11.4	12.9	5.5	20	11	4	CO_2 at detection limit, Cr, Co, Ni, Sm, Gd, Be, N, Li, B: Stripa Granite (Andrews et al. 1989)
DH-12	272.60	72.50	0.20	13.46	1.86	1.39	0.06	0.24	1.46	3.32	5.09	0.04	98.48	0.17	21.6	3.6	0.001	200	440	1.7	0.7	8	11.4	12.9	5.5	20	11	4	CO_2 at detection limit, Cr, Co, Ni, Sm, Gd, Be, N, Li, B: Stripa Granite (Andrews et al. 1989)
DH-12	289.48	N.R.	N.R.	N.R.	N.R.	N.R.	N.R.	N.R.	N.R.	N.R.	N.R.	N.R.	N.R.	N.R.	8.9	2.3	0.001	200	440	1.7	0.7	8	11.4	12.9	5.5	20	11	4	CO_2 at detection limit, Cr, Co, Ni, Sm, Gd, Be, N, Li, B: Stripa Granite (Andrews et al. 1989)
DH-12	301.18	75.46	0.21	11.91	2.27	1.57	0.07	0.36	1.54	3.03	3.75	0.06	98.98	0.13	18.6	3.4	0.001	200	440	1.7	0.7	8	11.4	12.9	5.5	20	11	4	CO_2 at detection limit, Cr, Co, Ni, Sm, Gd, Be, N, Li, B: Stripa Granite (Andrews et al. 1989)
DH-12	314.45	N.R.	N.R.	N.R.	N.R.	N.R.	N.R.	N.R.	N.R.	N.R.	N.R.	N.R.	N.R.	N.R.	12.1	2.0	0.001	200	440	1.7	0.7	8	11.4	12.9	5.5	20	11	4	CO_2 at detection limit, Cr, Co, Ni, Sm, Gd, Be, N, Li, B: Stripa Granite (Andrews et al. 1989)
DH-12	330.40	74.75	0.20	12.53	2.05	1.48	0.06	0.23	1.49	3.04	4.08	0.07	98.71	0.12	16.0	2.2	0.001	200	440	1.7	0.7	8	11.4	12.9	5.5	20	11	4	CO_2 at detection limit, Cr, Co, Ni, Sm, Gd, Be, N, Li, B: Stripa Granite (Andrews et al. 1989)
DH-12	348.65	N.R.	N.R.	N.R.	N.R.	N.R.	N.R.	N.R.	N.R.	N.R.	N.R.	N.R.	N.R.	N.R.	8.5	1.5	0.001	200	440	1.7	0.7	8	11.4	12.9	5.5	20	11	4	CO_2 at detection limit, Cr, Co, Ni, Sm, Gd, Be, N, Li, B: Stripa Granite (Andrews et al. 1989)
DH-12	369.95	73.51	0.22	12.93	2.32	1.18	0.08	0.31	1.66	3.27	3.99	0.16	98.80	0.23	15.0	4.2	0.001	200	440	1.7	0.7	8	11.4	12.9	5.5	20	11	4	CO_2 at detection limit, Cr, Co, Ni, Sm, Gd, Be, N, Li, B: Stripa Granite (Andrews et al. 1989)
DH-12	420.15	73.67	0.20	13.36	2.16	1.81	0.07	0.27	1.51	3.43	4.29	0.05	99.35	0.21	27.7	5.5	0.001	200	440	1.7	0.7	8	11.4	12.9	5.5	20	11	4	CO_2 at detection limit, Cr, Co, Ni, Sm, Gd, Be, N, Li, B: Stripa Granite (Andrews et al. 1989)
DH-12	435.80	71.11	0.22	13.67	2.06	1.48	0.08	0.21	1.61	3.67	5.04	0.07	98.08	0.26	16.3	3.9	0.001	200	440	1.7	0.7	8	11.4	12.9	5.5	20	11	4	CO_2 at detection limit, Cr, Co, Ni, Sm, Gd, Be, N, Li, B: Stripa Granite (Andrews et al. 1989)
DH-12	450.25	74.38	0.18	12.96	1.83	1.24	0.06	0.19	1.38	3.04	4.60	0.06	98.93	0.16	15.0	2.8	0.001	200	440	1.7	0.7	8	11.4	12.9	5.5	20	11	4	CO_2 at detection limit, Cr, Co, Ni, Sm, Gd, Be, N, Li, B: Stripa Granite (Andrews et al. 1989)
DH-12	465.25	72.04	0.20	13.84	2.05	1.48	0.08	0.31	1.37	3.27	5.11	0.05	99.04	0.52	12.2	8.9	0.001	200	440	1.7	0.7	8	11.4	12.9	5.5	20	11	4	CO_2 at detection limit, Cr, Co, Ni, Sm, Gd, Be, N, Li, B: Stripa Granite (Andrews et al. 1989)
DH-12	479.85	75.01	0.19	12.47	1.94	1.68	0.07	0.25	1.35	3.14	4.33	0.04	99.07	0.16	17.2	2.5	0.001	200	440	1.7	0.7	8	11.4	12.9	5.5	20	11	4	CO_2 at detection limit, Cr, Co, Ni, Sm, Gd, Be, N, Li, B: Stripa Granite (Andrews et al. 1989)
MIU-4	97.42	76.57	0.08	12.77	0.08	1.04	0.04	0.09	0.60	3.18	3.81	0.02	N.R.	0.36	20.60	2.34	0.001	1	76.79	5.21	4.22	1.93	4.54	4.99	3.17	1.00E-06	13.63	1.00E-06	CO_2 at detection limit, negligible N and B
MIU-4	140.87	76.14	0.08	12.55	0.09	0.98	0.05	0.03	0.71	3.44	4.37	0.02	N.R.	0.34	24.20	3.00	0.000	1	125.99	1.01	4.17	1.00	1.00E-06	1.00E-06	3.87	1.00E-06	25.57	1.00E-06	CO_2 at detection limit, negligible Sm, Gd, N and B
MIU-4	289.75	72.94	0.13	13.49	0.23	1.65	0.08	0.06	0.99	3.49	4.96	0.02	N.R.	0.45	18.39	1.88	0.000	1	1.38E+03	0.60	2.87	0.59	1.00E-06	1.00E-06	4.54	1.00E-06	37.10	1.00E-06	CO_2 at detection limit, negligible Sm, Gd, N and B
MIU-4	340.12	73.52	0.13	13.20	0.29	1.56	0.08	0.11	1.11	3.52	4.67	0.04	N.R.	0.27	29.73	5.15	0.000	1	1.17E+03	0.81	4.08	0.35	1.00E-06	1.00E-06	3.62	1.00E-06	39.57	1.00E-06	CO_2 at detection limit, negligible Sm, Gd, N and B
MIU-4	48.11	69.63	0.07	14.52	2.34	0.68	0.02	0.38	0.55	1.69	4.56	0.13	N.R.	4.10	60.73	38.96	0.359	1	1.02E+03	7.39	6.69	6.69	1.00E-06	1.00E-06	5.32	1.00E-06	33.41	1.00E-06	Negligible Sm, Gd, N and B
MIU-4	96.255	73.51	0.11	12.72	1.90	1.27	0.18	0.15	0.94	3.55	4.29	0.02	N.R.	0.91	28.80	20.14	0.121	1	572.72	2.42	2.74	4.08	1.00E-06	1.00E-06	3.22	1.00E-06	25.17	1.00E-06	Negligible Sm, Gd, N and B
MIU-4	116.395	77.30	0.06	13.00	0.81	0.17	0.00	0.09	0.09	0.07	5.79	0.01	N.R.	1.80	20.74	4.98	0.121	1	1241.99	1.34	0.10	1.95	6.07	7.56	1.85	1.00E-06	21.78	1.00E-06	Co at detection limit, negligible N and B
MIU-4	117.11	75.37	0.05	13.20	1.18	0.33	0.01	0.16	0.17	0.06	4.72	0.01	N.R.	2.60	19.37	4.16	0.154	1	1516.02	0.61	0.10	0.51	6.49	7.66	3.28	1.00E-06	42.16	1.00E-06	Negligible N and B
MIU-4	117.27	78.66	0.06	12.60	1.00	0.28	0.01	0.11	0.14	0.07	4.75	0.01	N.R.	2.10	18.49	4.48	0.202	1	1345.09	0.51	0.15	1.21	5.90	6.42	2.59	1.00E-06	40.70	1.00E-06	Negligible N and B
MIU-4	118.1	76.05	0.07	13.29	1.08	0.38	0.01	0.12	0.12	1.66	5.66	0.01	N.R.	1.60	23.03	9.75	0.110	1	793.86	1.80	1.83	0.68	1.66	2.90	1.91	1.00E-06	9.51	1.00E-06	Negligible N and B
MIU-4	97.42	76.57	0.08	12.77	0.08	1.04	0.04	0.09	0.60	3.18	3.81	0.02	N.R.	0.36	20.60	2.34	0.001	200	76.79	5.21	4.22	1.93	4.54	4.99	3.17	1.00E-06	13.63	1.00E-06	CO_2 and Cl at detection limit, negligible N and B
MIU-4	140.87	76.14	0.08	12.55	0.09	0.98	0.05	0.03	0.71	3.44	4.37	0.02	N.R.	0.34	24.20	3.00	0.000	200	125.99	1.01	4.17	1.00	1.00E-06	1.00E-06	3.87	1.00E-06	25.57	1.00E-06	CO_2 and Cl set at detection limit, negligible Sm, Gd, N and B
MIU-4	289.75	72.94	0.13	13.49	0.23	1.65	0.08	0.06	0.99	3.49	4.96	0.02	N.R.	0.45	18.39	1.88	0.000	200	1377.09	0.60	2.87	0.59	1.00E-06	1.00E-06	4.54	1.00E-06	37.10	1.00E-06	CO_2 and Cl set at detection limit, negligible Sm, Gd, N and B
MIU-4	340.12	73.52	0.13	13.20	0.29	1.56	0.08	0.11	1.11	3.52	4.67	0.04	N.R.	0.27	29.73	5.15	0.000	200	1171.72	0.81	4.08	0.35	1.00E-06	1.00E-06	3.62	1.00E-06	39.57	1.00E-06	CO_2 and Cl set at detection limit, negligible Sm, Gd, N and B
MIU-4	48.11	69.63	0.07	14.52	2.34	0.68	0.02	0.38	0.55	1.69	4.56	0.13	N.R.	4.10	60.73	38.96	0.359	200	1018.82	7.39	6.69	6.69	1.00E-06	1.00E-06	5.32	1.00E-06	33.41	1.00E-06	Cl set at detection limit, negligible Sm, Gd, N and B
MIU-4	96.255	73.51	0.11	12.72	1.90	1.27	0.18	0.15	0.94	3.55	4.29	0.02	N.R.	0.91	28.80	20.14	0.121	200	572.72	2.42	2.74	4.08	1.00E-06	1.00E-06	3.22	1.00E-06	25.17	1.00E-06	Cl set at detection limit, negligible Sm, Gd, N and B
MIU-4	116.395	77.30	0.06	13.00	0.81	0.17	0.00	0.09	0.09	0.07	5.79	0.01	N.R.	1.80	20.74	4.98	0.121	200	1241.99	1.34	0.10	1.95	6.07	7.56	1.85	1.00E-06	21.78	1.00E-06	Cl and Co at detection limit, negligible N and B
MIU-4	117.11	75.37	0.05	13.20	1.18	0.33	0.01	0.16	0.17	0.06	4.72	0.01	N.R.	2.60	19.37	4.16	0.154	200	1516.02	0.61	0.10	0.51	6.49	7.66	3.28	1.00E-06	42.16	1.00E-06	Cl set at detection limit, negligible N and B
MIU-4	117.27	78.66	0.06	12.60	1.00	0.28	0.01	0.11	0.14	0.07	4.75	0.01	N.R.	2.10	18.49	4.48	0.202	200	1345.09	0.51	0.15	1.21	5.90	6.42	2.59	1.00E-06	40.70	1.00E-06	Cl set at detection limit, negligible N and B
MIU-4	118.1	76.05	0.07	13.29	1.08	0.38	0.01	0.12	0.12	1.66	5.66	0.01	N.R.	1.60	23.03	9.75	0.110	200	793.86	1.80	1.83	0.68	1.66	2.90	1.91	1.00E-06	9.51	1.00E-06	Cl set at detection limit, negligible N and B
MIU-4	97.42	76.57	0.08	12.77	0.08	1.04	0.04	0.09	0.60	3.18	3.81	0.02	N.R.	0.36	20.60	2.34	0.001	1	76.79	5.21	4.22	1.93	4.54	4.99	3.17	20	13.63	4.00	CO_2 at detection limit, N and B from Stripa Granite
MIU-4	140.87	76.14	0.08	12.55	0.09	0.98	0.05	0.03	0.71	3.44	4.37	0.02	N.R.	0.34	24.20	3.00	0.000	1	125.99	1.01	4.17	1.00	11.4	12.9	3.87	20	25.57	4.00	CO_2 at detection limit, Sm, Gd, N and B from Stripa Granite
MIU-4	289.75	72.94	0.13	13.49	0.23	1.65	0.08	0.06	0.99	3.49	4.96	0.02	N.R.	0.45	18.39	1.88	0.000	1	1377.09	0.60	2.87	0.59	11.4	12.9	4.54	20	37.10	4.00	CO_2 at detection limit, Sm, Gd, N and B from Stripa Granite
MIU-4	340.12	73.52	0.13	13.20	0.29	1.56	0.08	0.11	1.11	3.52	4.67	0.04	N.R.	0.27	29.73	5.15	0.000	1	1171.72	0.81	4.08	0.35	11.4	12.9	3.62	20	39.57	4.00	CO_2 at detection limit, Sm, Gd, N and B from Stripa Granite
MIU-4	48.11	69.63	0.07	14.52	2.34	0.68	0.02	0.38	0.55	1.69	4.56	0.13	N.R.	4.10	60.73	38.96	0.359	1	1018.82	7.39	6.69	6.69	11.4	12.9	5.32	20	33.41	4.00	Sm, Gd, N and B from Stripa Granite
MIU-4	96.255	73.51	0.11	12.72	1.90	1.27	0.18	0.15	0.94	3.55	4.29	0.02	N.R.	0.91	28.80	20.14	0.121	1	572.72	2.42	2.74	4.08	11.4	12.9	3.22	20	25.17	4.00	Sm, Gd, N and B from Stripa Granite
MIU-4	116.395	77.30	0.06	13.00	0.81	0.17	0.00	0.09	0.09	0.07	5.79	0.01	N.R.	1.80	20.74	4.98	0.121	1	1241.99	1.34	0.10	1.95	6.07	7.56	1.85	20	21.78	4.00	Co at detection limit, N and B from Stripa Granite
MIU-4	117.11	75.37	0.05	13.20	1.18	0.33	0.01	0.16	0.17	0.06	4.72	0.01	N.R.	2.60	19.37	4.16	0.154	1	1516.02	0.61	0.10	0.51	6.49	7.66	3.28	20	42.16	4.00	N and B from Stripa Granite
MIU-4	117.27	78.66	0.06	12.60	1.00	0.28	0.01	0.11	0.14	0.07	4.75	0.01	N.R.	2.10	18.49	4.48	0.202	1	1345.09	0.51	0.15	1.21	5.90	6.42	2.59	20	40.70	4.00	N and B from Stripa Granite
MIU-4	118.1	76.05	0.07	13.29	1.08	0.38	0.01	0.12	0.12	1.66	5.66	0.01	N.R.	1.60	23.03	9.75	0.110	1	793.86	1.80	1.83	0.68	1.66	2.90	1.91	20	9.51	4.00	N and B from Stripa Granite
MIU-4	97.42	76.57	0.08	12.77	0.08	1.04	0.04	0.09	0.60	3.18	3.81	0.02	N.R.	0.36	20.60	2.34	0.001	200	76.79	5.21	4.22	1.93	4.54	4.99	3.17	20	13.63	4.00	CO_2 and Cl at detection limit, N and B from Stripa Granite
MIU-4	140.87	76.14	0.08	12.55	0.09	0.98	0.05	0.03	0.71	3.44	4.37	0.02	N.R.	0.34	24.20	3.00	0.000	200	125.99	1.01	4.17	1.00	11.4	12.9	3.87	20	25.57	4.00	CO_2 and Cl at detection limit, Sm, Gd, N and B from Stripa Granite
MIU-4	289.75	72.94	0.13	13.49	0.23	1.65	0.08	0.06	0.99	3.49	4.96	0.02	N.R.	0.45	18.39	1.88	0.000	200	1377.09	0.60	2.87	0.59	11.4	12.9	4.54	20	37.10	4.00	CO_2 and Cl at detection limit, Sm, Gd, N and B from Stripa Granite
MIU-4	340.12	73.52	0.13	13.20	0.29	1.56	0.08	0.11	1.11	3.52	4.67	0.04	N.R.	0.27	29.73	5.15	0.000	200	1171.72	0.81	4.08	0.35	11.4	12.9	3.62	20	39.57	4.00	CO_2 and Cl at detection limit, Sm, Gd, N and B from Stripa Granite
MIU-4	48.11	69.63	0.07	14.52	2.34	0.68	0.02	0.38	0.55	1.69	4.56	0.13	N.R.	4.10	60.73	38.96	0.359	200	1018.82	7.39	6.69	6.69	11.4	12.9	5.32	20	33.41	4.00	Cl at detection limit, Sm, Gd, N and B from Stripa Granite
MIU-4	96.255	73.51	0.11	12.72	1.90	1.27	0.18	0.15	0.94	3.55	4.29	0.02	N.R.	0.91	28.80	20.14	0.121	200	572.72	2.42	2.74	4.08	11.4	12.9	3.22	20	25.17	4.00	Cl at detection limit, Sm, Gd, N and B from Stripa Granite
MIU-4	116.395	77.30	0.06	13.00	0.81	0.17	0.00	0.09	0.09	0.07	5.79	0.01	N.R.	1.80	20.74	4.98	0.121	200	1241.99	1.34	0.10	1.95	6.07	7.56	1.85	20	21.78	4.00	Cl and Co at detection limit, N and B from Stripa Granite
MIU-4	117.11	75.37	0.05	13.20	1.18	0.33	0.01	0.16	0.17	0.06	4.72	0.01	N.R.	2.60	19.37	4.16	0.154	200	1516.02	0.61	0.10	0.51	6.49	7.66	3.28	20	42.16	4.00	Cl at detection limit, N and B from Stripa Granite
MIU-4	117.27	78.66	0.06	12.60	1.00	0.28	0.01	0.11	0.14	0.07	4.75	0.01	N.R.	2.10	18.49	4.48	0.202	200	1345.09	0.51	0.15	1.21	5.90	6.42	2.59	20	40.70	4.00	Cl at detection limit, N and B from Stripa Granite
MIU-4	118.1	76.05	0.07	13.29	1.08	0.38	0.01	0.12	0.12	1.66	5.66	0.01	N.R.	1.60	23.03	9.75	0.110	200	793.86	1.80	1.83	0.68	1.66	2.90	1.91	20	9.51	4.00	Cl at detection limit, N and B from Stripa Granite
HDB-1	551.47	68.23	0.532	11.56	2.43	1.5	0.023	1.38	0.48	1.55	1.804	0.076	98.06	5.94	7.39	2.57	0.001	1	1.00E-06	1.00E-06	1.00E-06	1.00E-06	3.31	3.15	1.00E-06	6.00E+02	1.00E-06	1.00E-06	No data for C, Cl, F, Cr, Co, Ni, Be, N, Li, B, pelagic shale values used from Taylor and McLennan
HDB-1	556.425	73.49	0.396	8.82	2.06	0.81	0.020	0.93	0.46	1.34	1.346	0.059	96.49	5.76	7.39	2.57	0.001	1	1.00E-06	1.00E-06	1.00E-06	1.00E-06	3.31	3.15	1.00E-06	6.00E+02	1.00E-06	1.00E-06	No data for trace elements, including U and Th. Therefore only major elements changed compared to values used in 551.42-551.52 m calculation
HDB-1	551.47	68.23	0.532	11.56	2.43	1.5	0.023	1.38	0.48	1.55	1.804	0.076	98.06	5.94	7.39	2.57	0.001	1	1300	90	74	230	3.31	3.15	2.6	600	57	230	No data for C, Cl, F, Cr, Co, Ni, Be, N, Li, B, pelagic shale values used from Taylor and McLennan
HDB-1	556.425	73.49	0.396	8.82	2.06	0.81	0.020	0.93	0.46	1.34	1.346	0.059	96.49	5.76	7.39	2.57	0.001	1	1300	90	74	230	3.31	3.15	2.6	600	57	230	No data for trace elements, including U and Th. Therefore only major elements changed compared to values used in 551.42-551.52 m calculation

Data sources:

DH12	Excel file 'rock_DH12', received from T. Iwatsuki of JNC on 26th January 2003
MIU-4	Excel file 'Rock REE' received from T Iwatsuki of JNC on 26th January 2003
MIU-4	Excel file 'Rock major&minor' which was received from T. Iwatsuki on 26th January 2003.
HDB-1	Paper tabulation received by R. Metcalfe from T. Kunimaru of JNC on 8th October 2002.